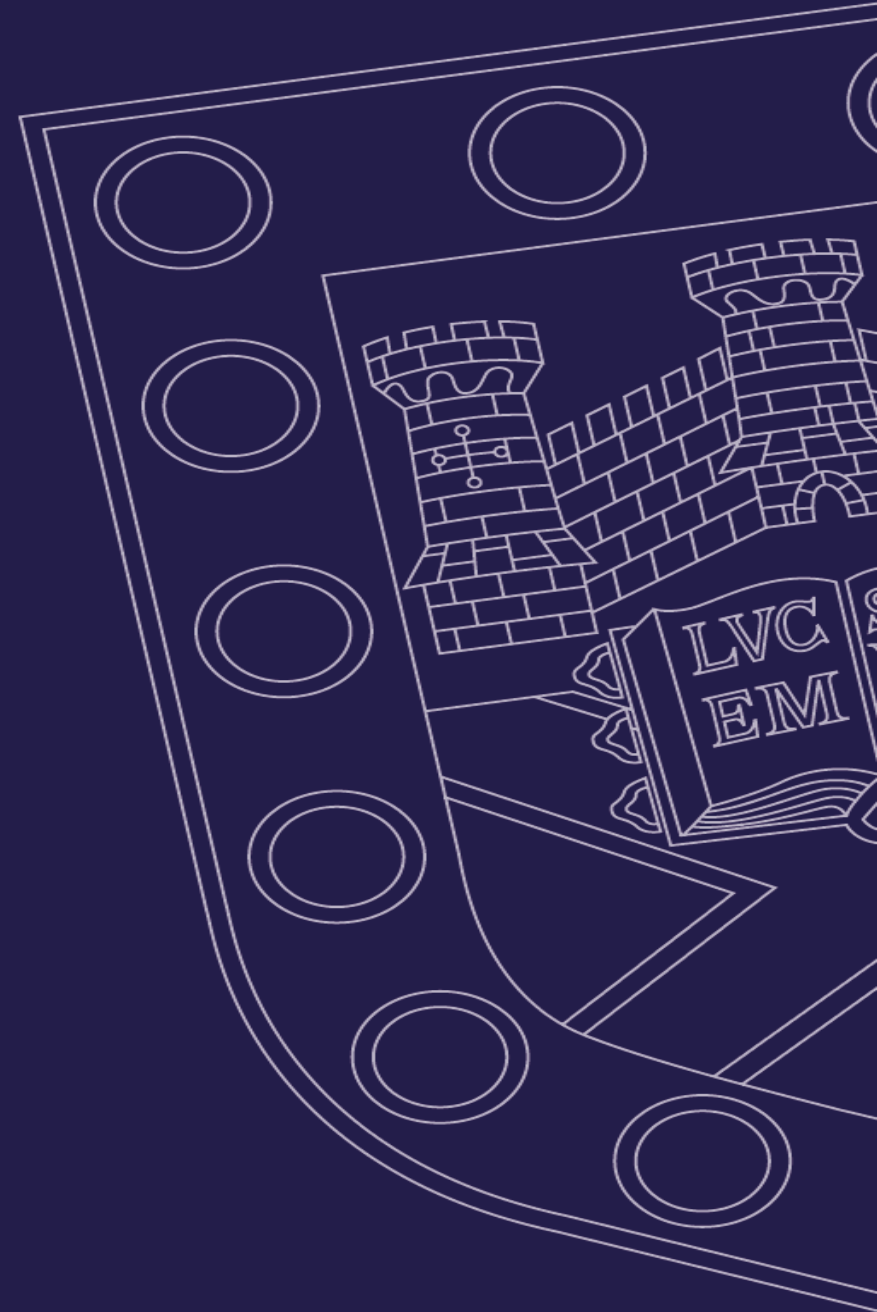


# Mechanistic Models of Deformation Twinning and Martensitic Transformations

Bob Pond

Acknowledge: John Hirth



# Classical Model (CM)

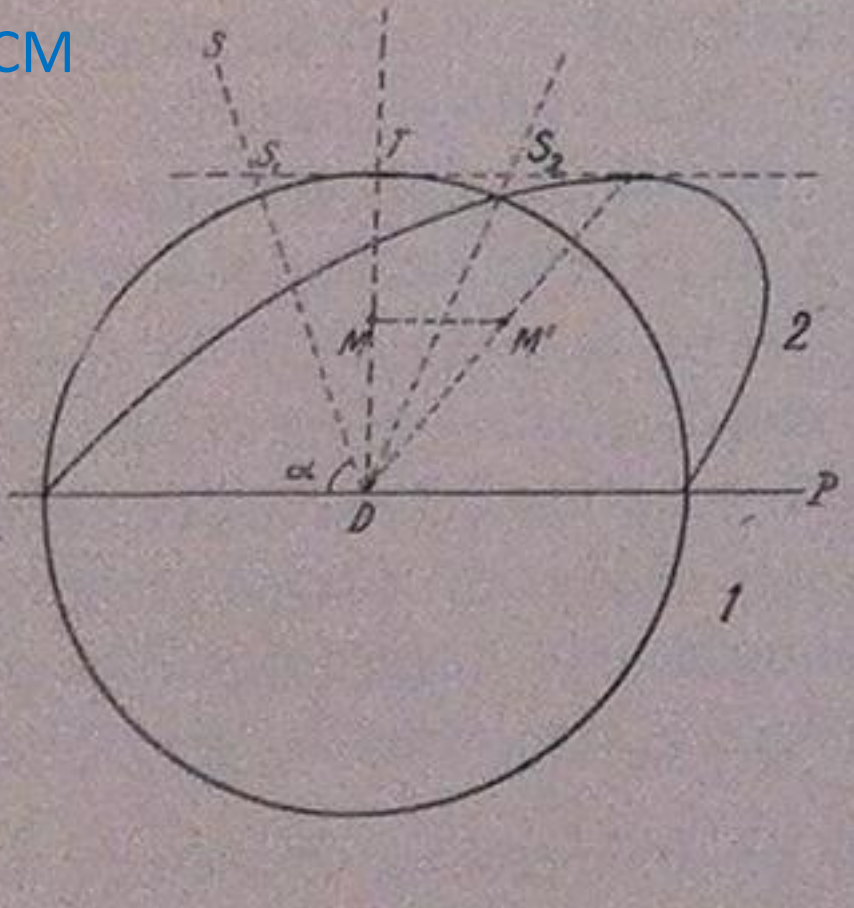
Geometrical  
– invariant plane

# Topological Model (TM)

Mechanistic  
– coherent interfaces, interfacial line-defects



CM

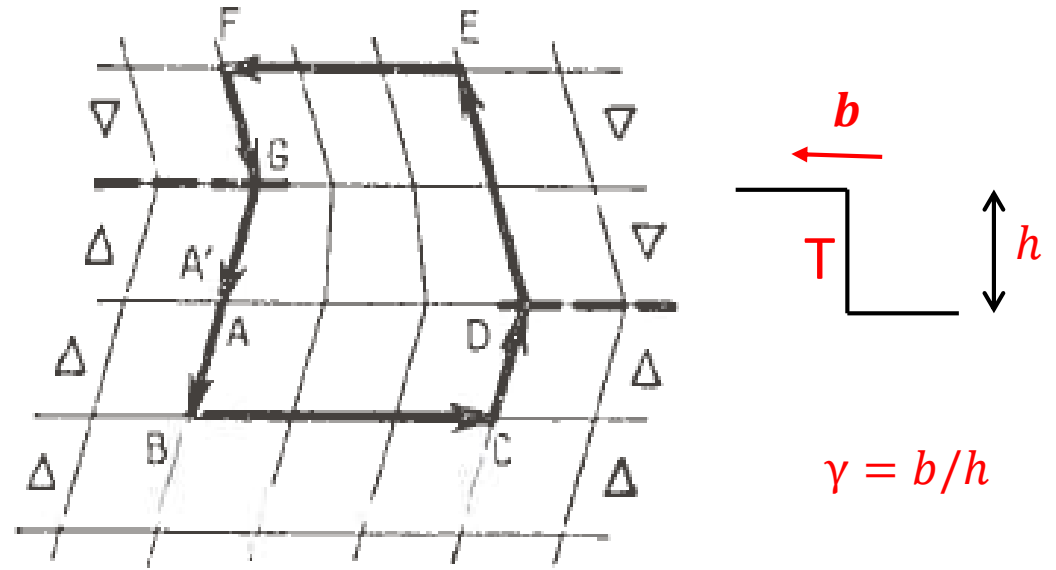


Twinning : e.g. G. Friedel, 1926

PTMC : WLR and BM, 1953

TM

s



Twinning dislocation: e.g. F.C. Frank, 1949  
(disconnection)

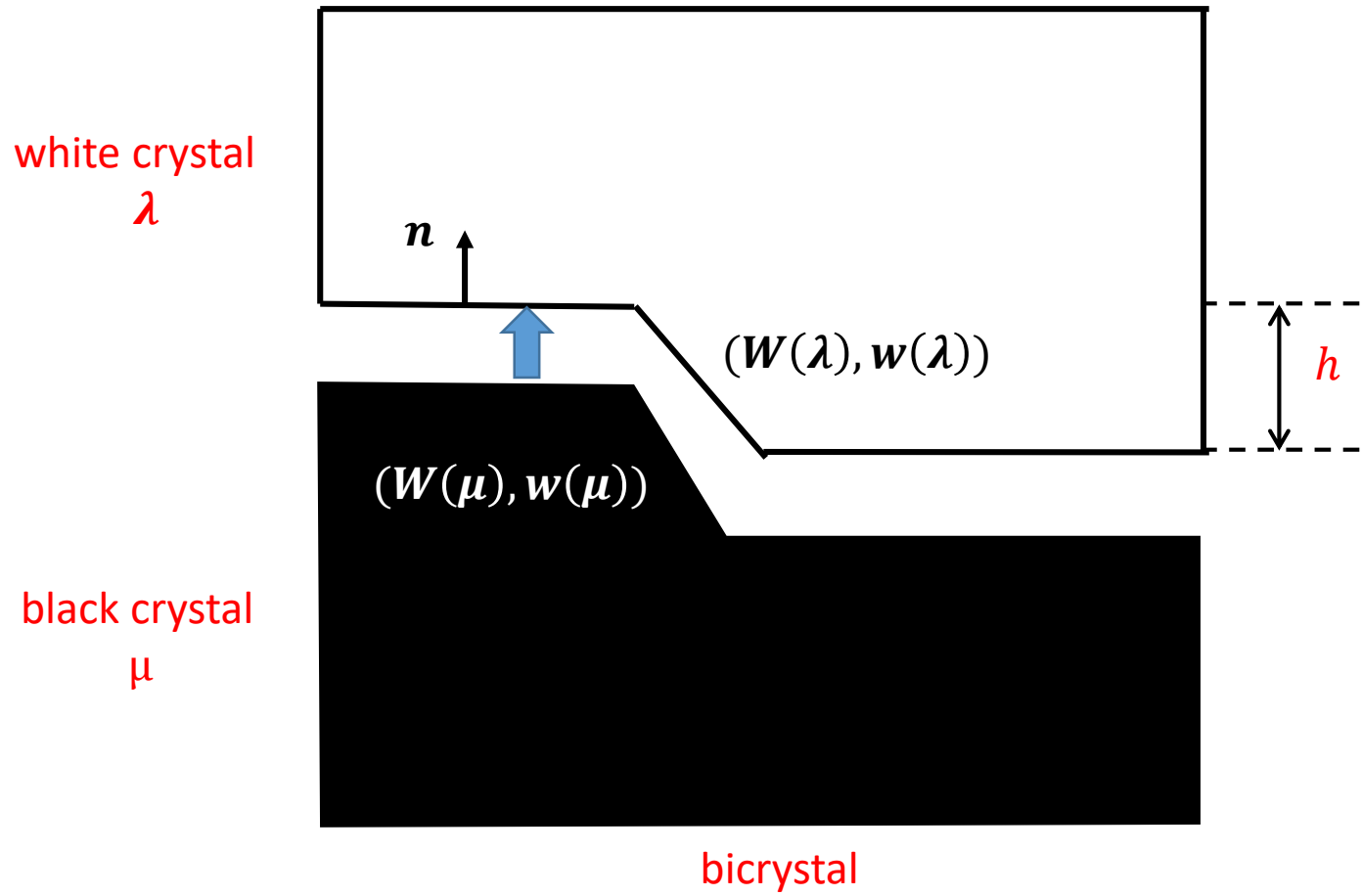
Bilby & Crocker, 1965

Martensitic Transformations  
Pond and Hirth, 2003



# Interfacial defect character and kinetics

# Admissible interfacial defects



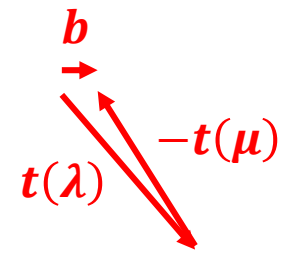
*Operation characterising defect*

$$(W(\lambda), w(\lambda))(W(\mu), w(\mu))^{-1}$$

*Interfacial dislocations*  
 $(I, b)$

*Twinning disconnections*  
 $b = t(\lambda) - Pt(\mu)$   
 $h = n \cdot t(\lambda)$

$$\gamma = b/h$$



Pond, 1989



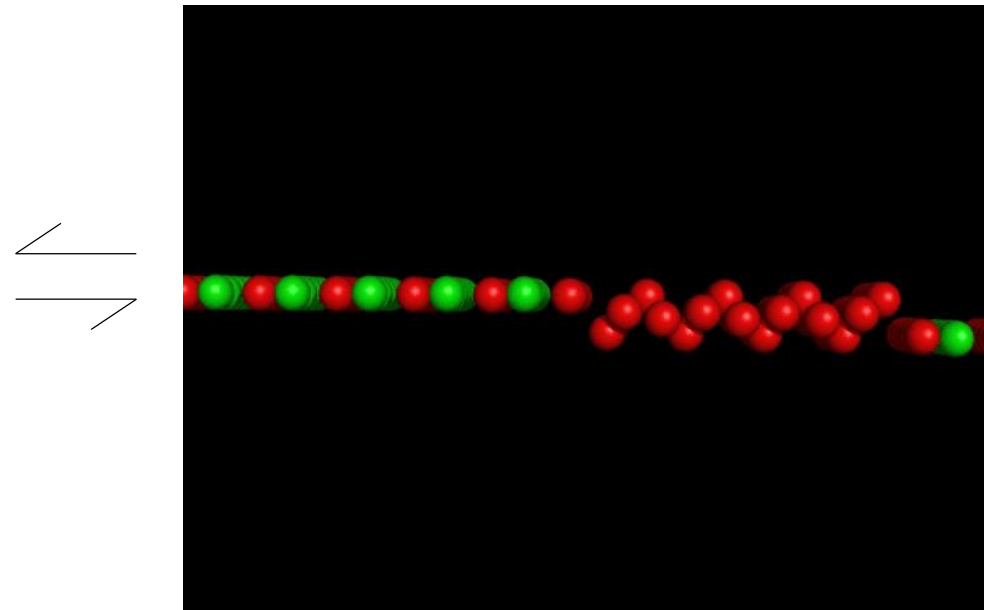
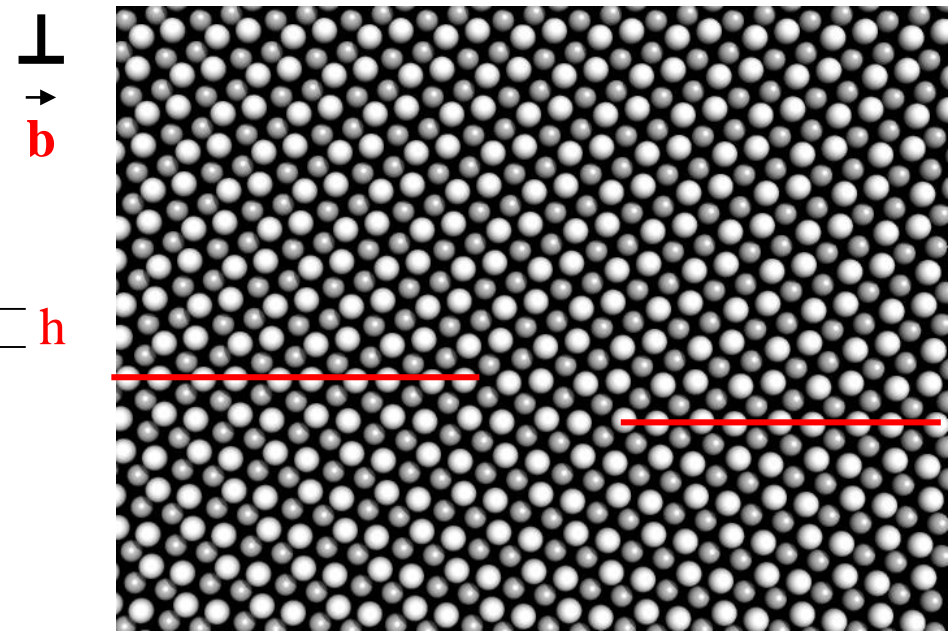
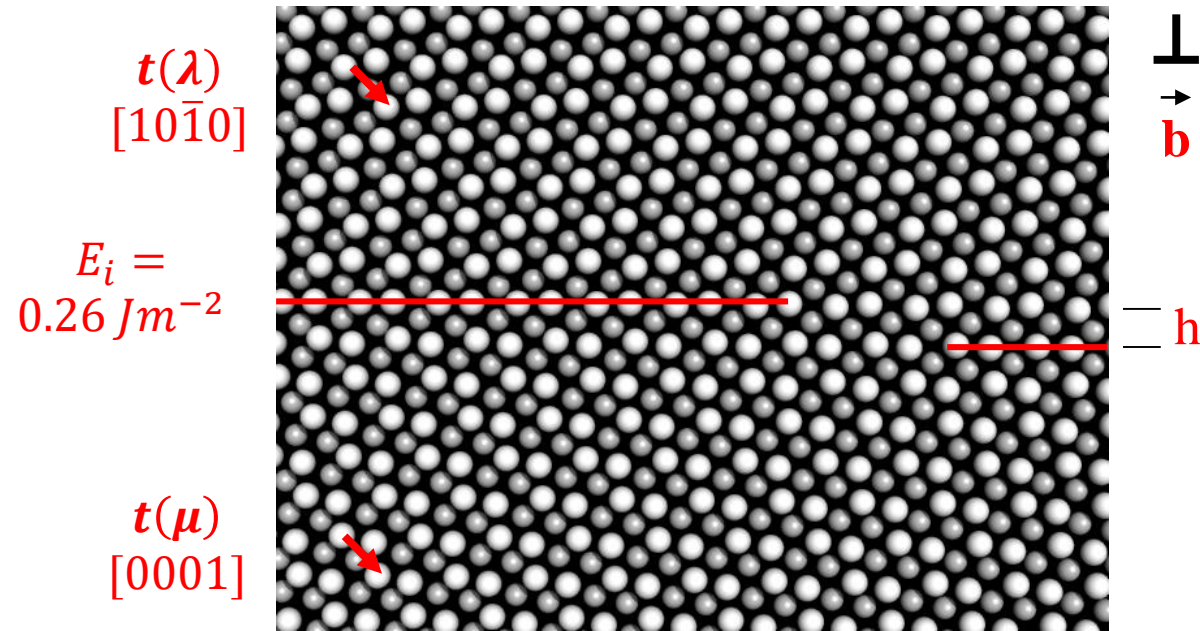
# Thermally activated disconnections

- activation energy at fixed stress  $\sim b^2$
- loop nucleation rate,  $\dot{N}$ , reasonable for small  $b$
- defect mobility,  $\dot{G}$
- enhanced by larger core width,  $w$ , which is promoted by small  $h$
- simple shuffles





# Motion of a twinning disconnection in a $(10\bar{1}2)$ twin



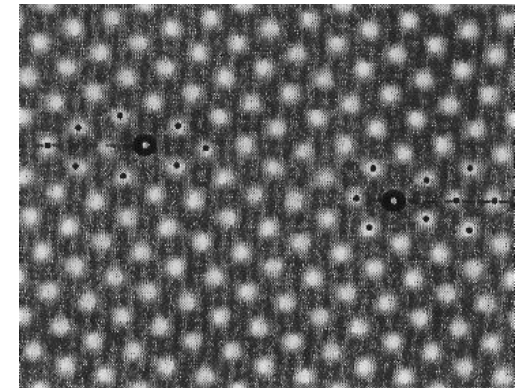
$$|\mathbf{b}| = 0.062 \text{ nm}$$

$$h = 2d_{(10\bar{1}2)} = 0.376 \text{ nm}$$

$$\gamma = b/h$$

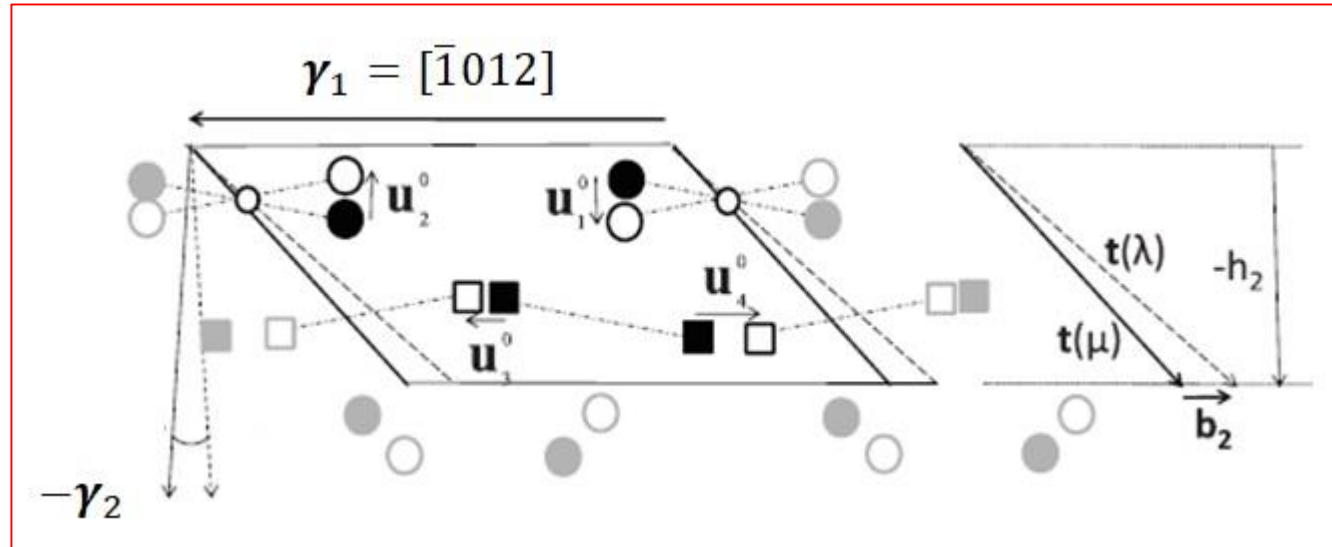
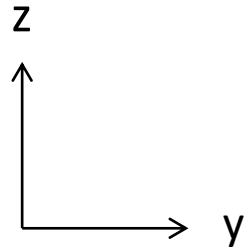
$$w \sim 6a$$

$$\sigma_p^d = 1 \text{ MPa}$$



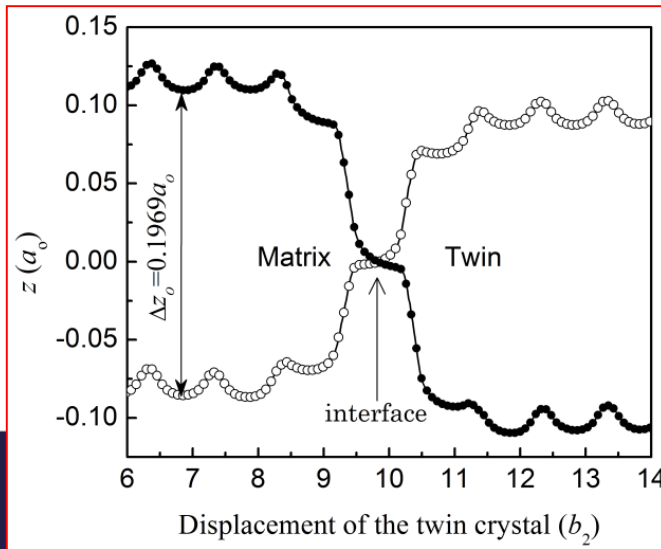
$\alpha - \text{Ti}$   
Braisaz et al. 1966

# Atom Tracking: Shear and Shuffle Displacements in $(10\bar{1}2)$ Twin

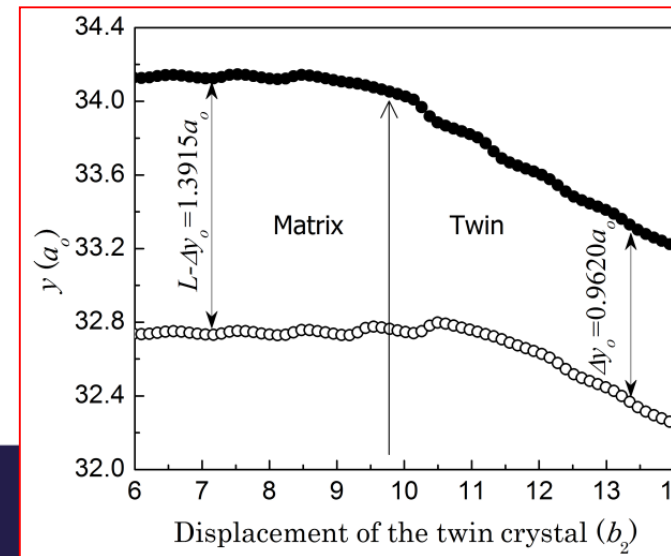


4 distinct atoms

“rocking”



“swapping”

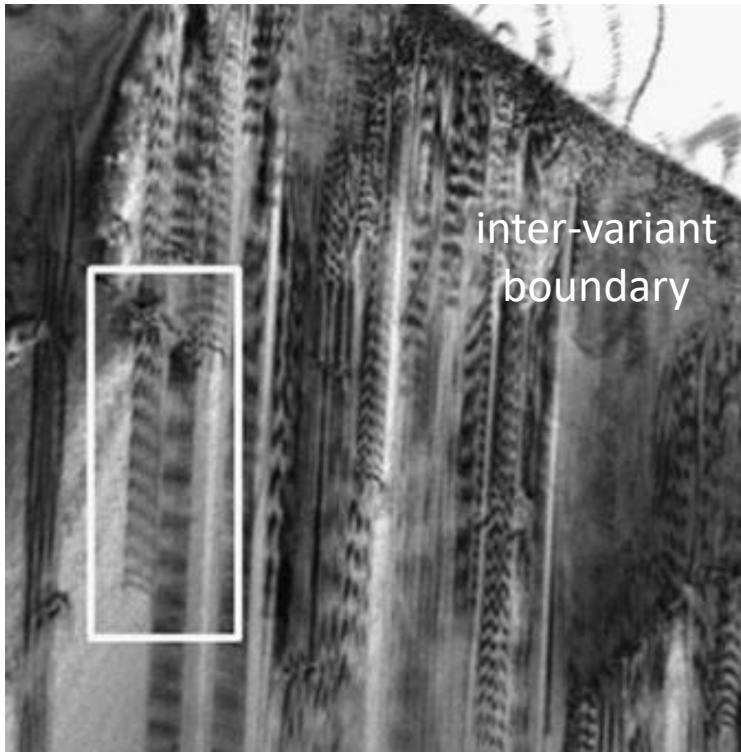


Pond et al., 2013





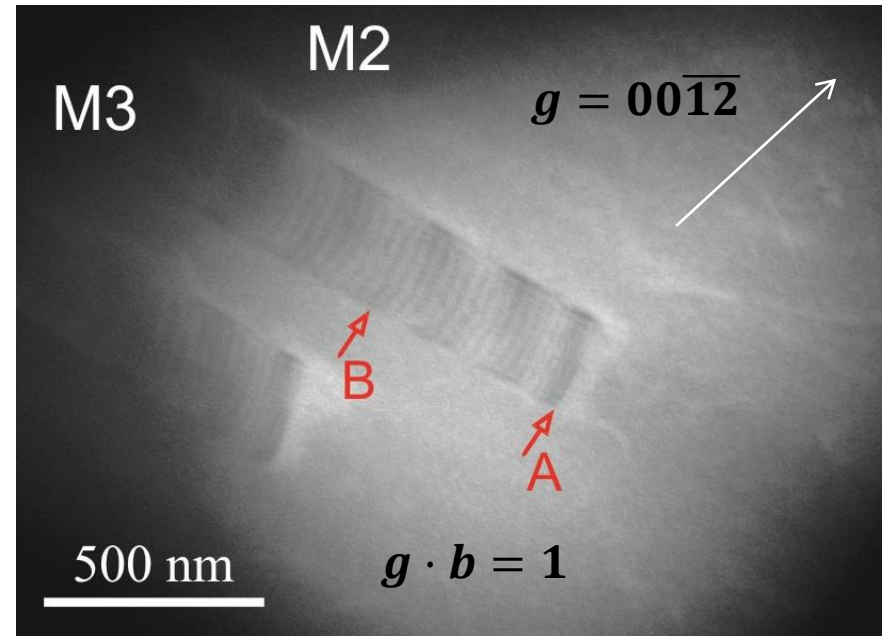
# Deformation twins in Ni<sub>2</sub>MnGa



0.5  $\mu\text{m}$

Pond et al. 2012

Zarubova et al. 2012



Disconnection

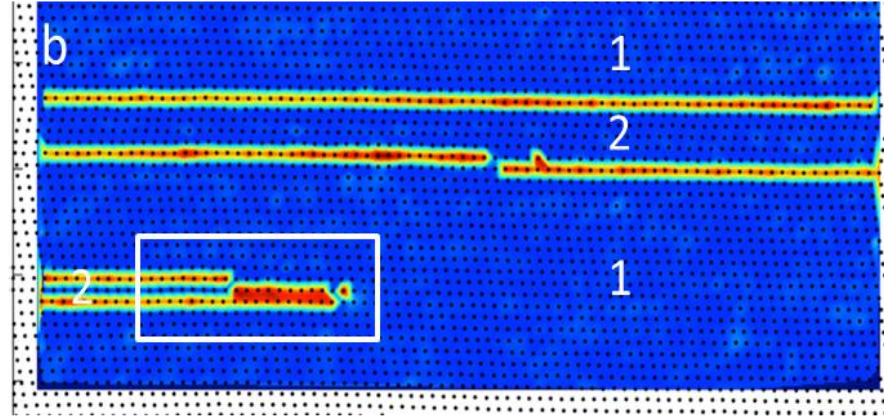
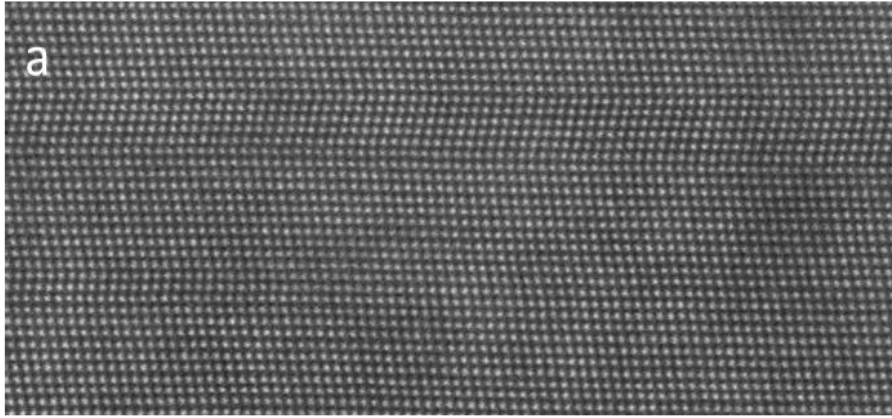
$$b = \frac{1}{12} [10\bar{1}] = 0.072 \text{ nm}$$

$$h = d_{(202)} = 0.211 \text{ nm}$$

$$\gamma = \frac{b}{h} = 0.34$$



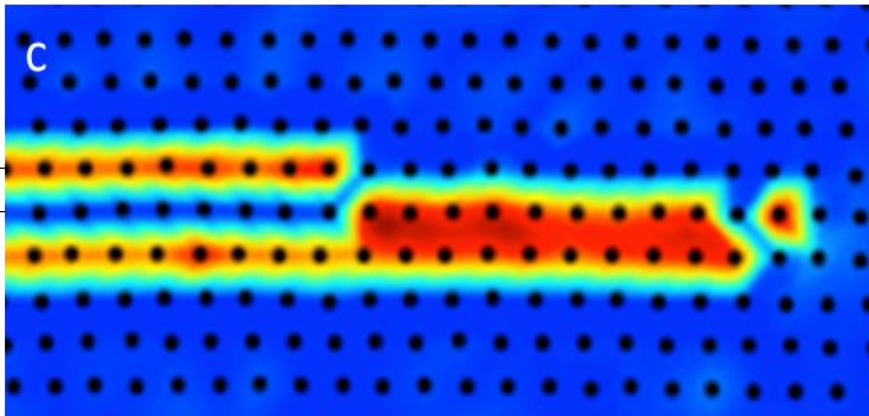
# Twin tip in Ni<sub>2</sub>MnGa



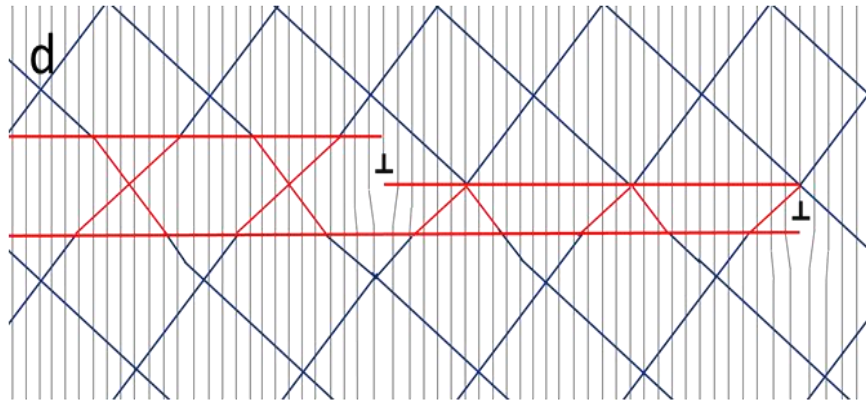
$$E_i = 0.01 \text{ Jm}^{-2}$$

4 distinct atoms

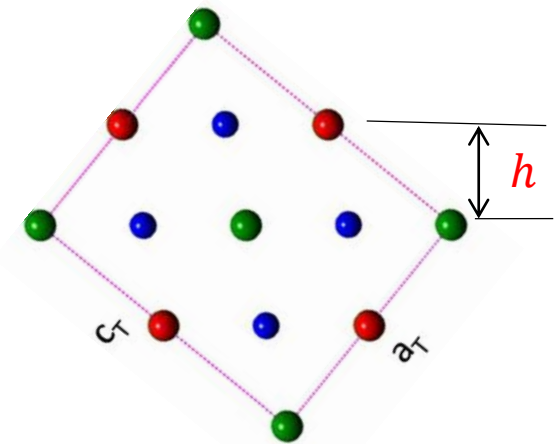
no shuffling



$$g = 20\bar{2}$$



Muntifering et al. 2014

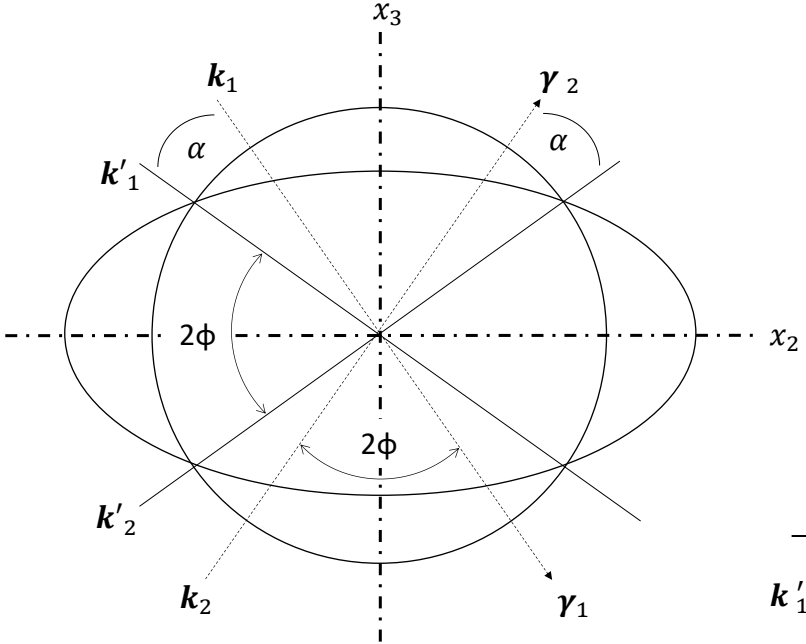
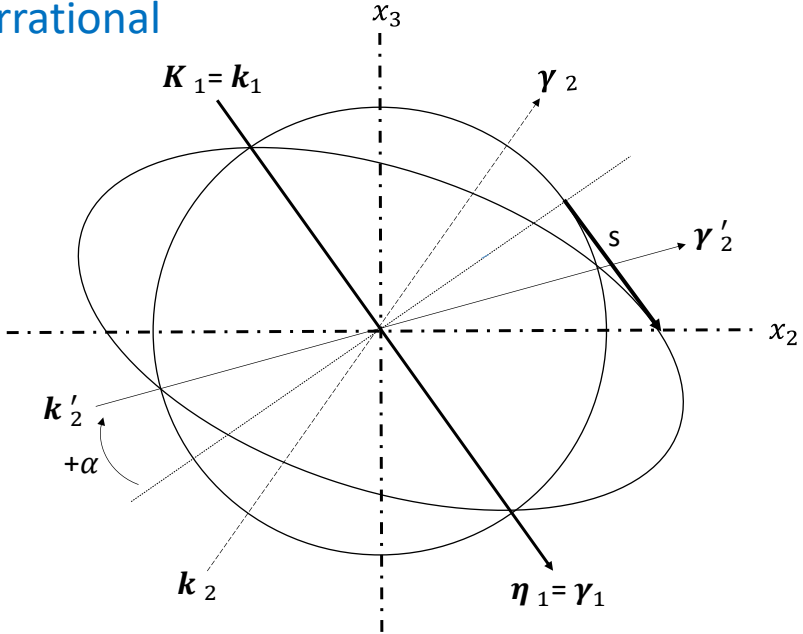


Topological model for type II twinning

# Classical Model: irrational plane of shear

Type I

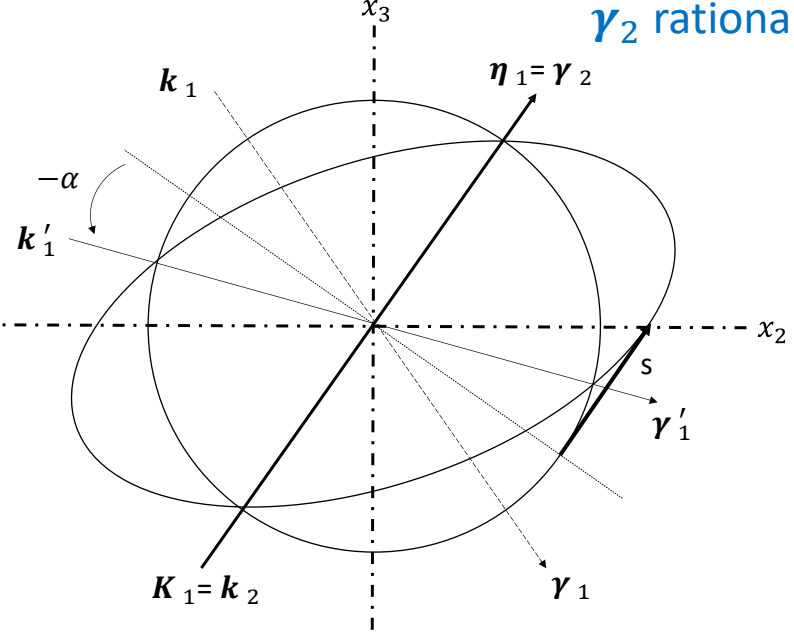
$k_1$  rational  
 $\gamma_1$  irrational



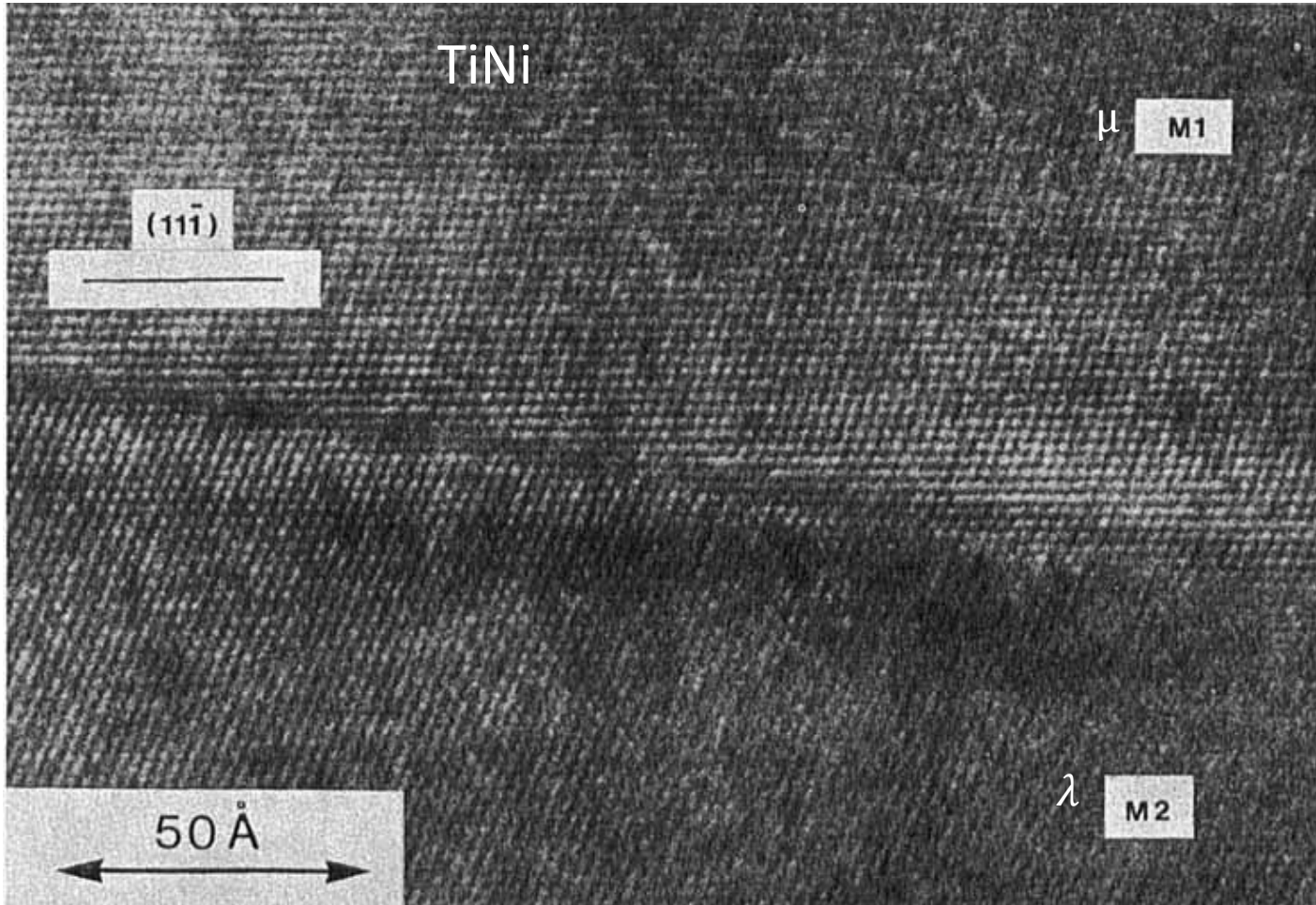
$$s = 2 \tan \alpha$$

Type II

$k_2$  irrational  
 $\gamma_2$  rational

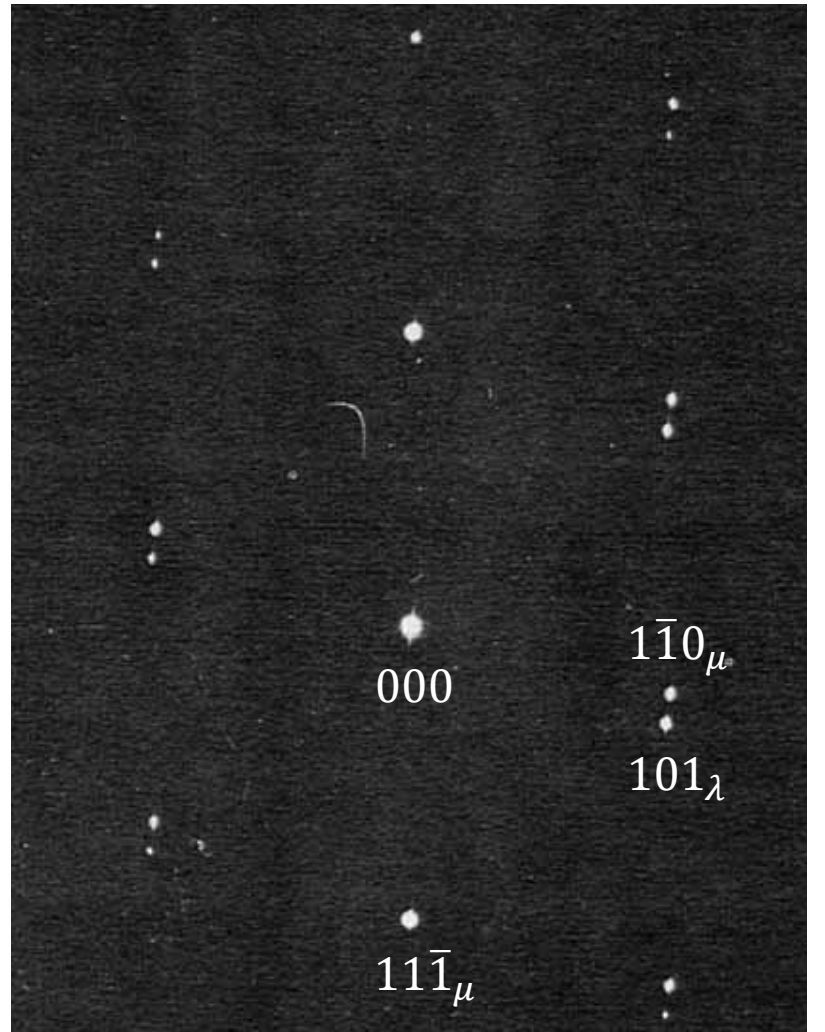






Knowles, 1982

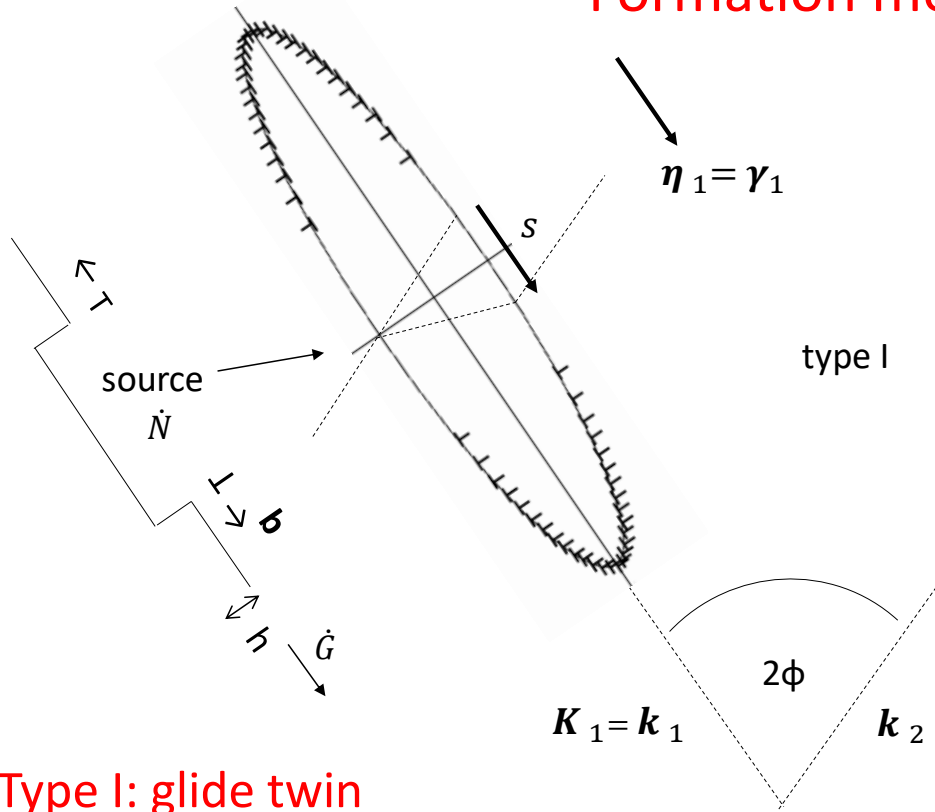
(a)



(b)



# Formation mechanisms for type I and II twins

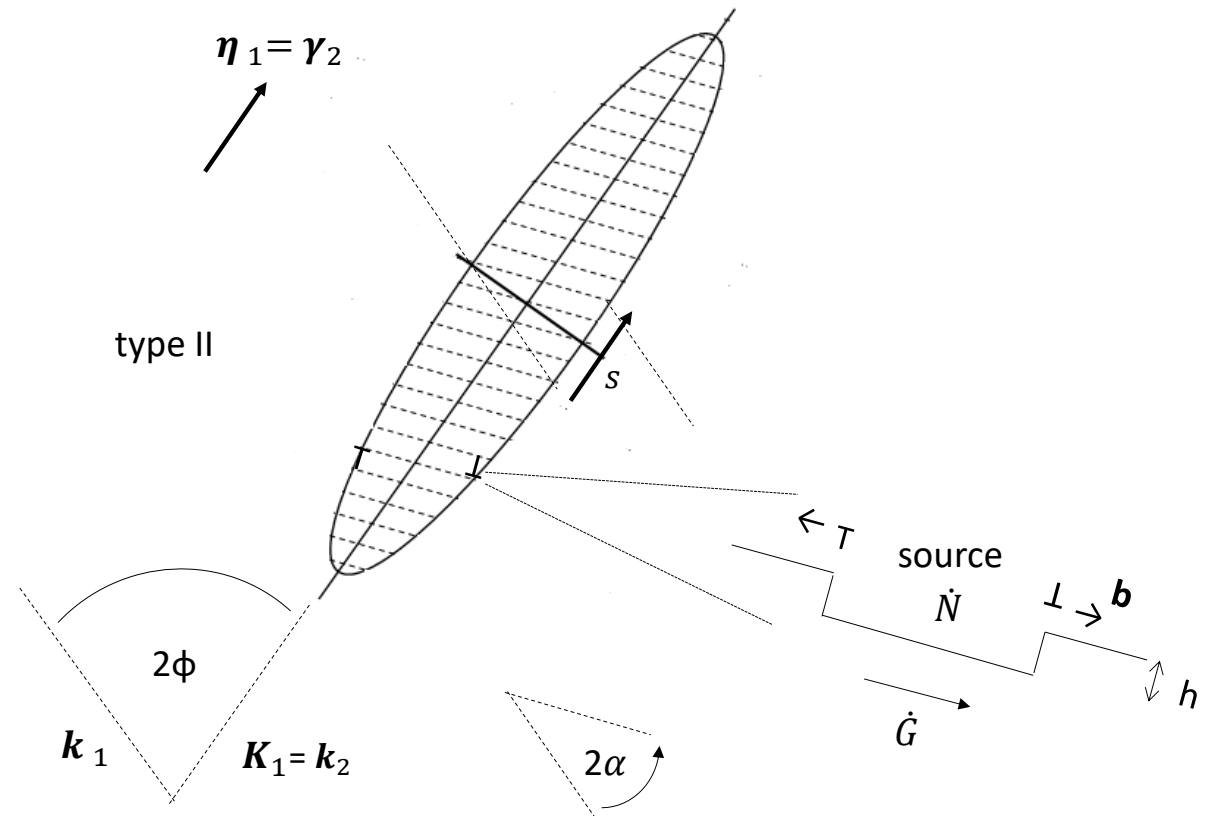


Type I: glide twin

$$\gamma = b/h$$

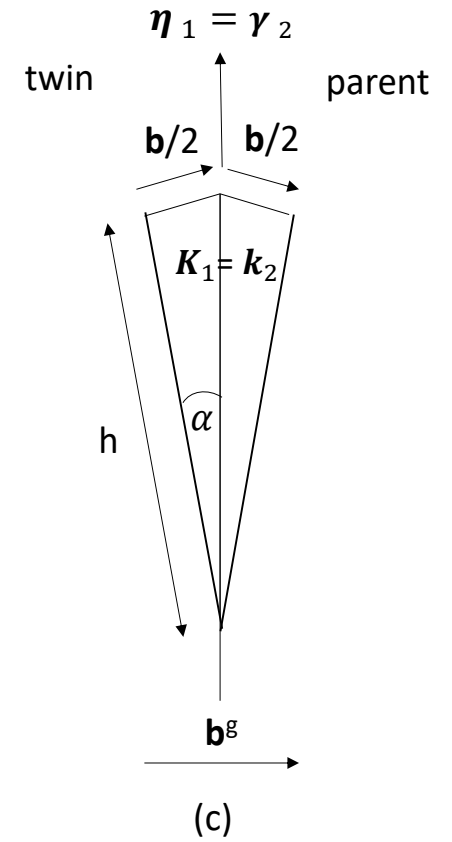
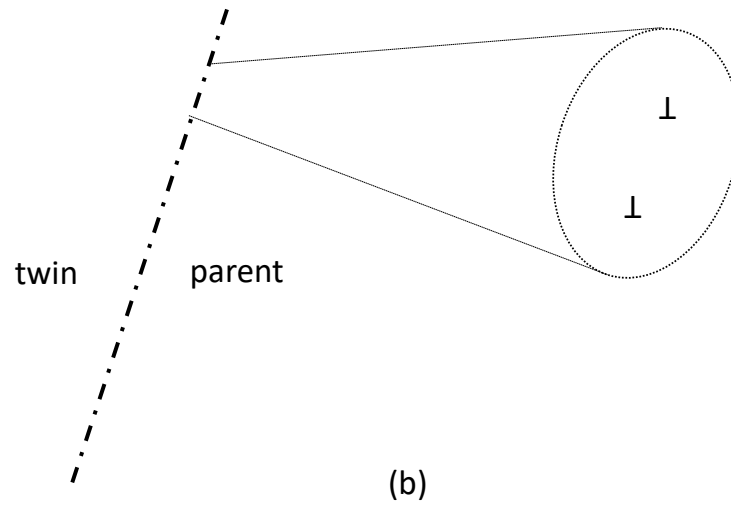
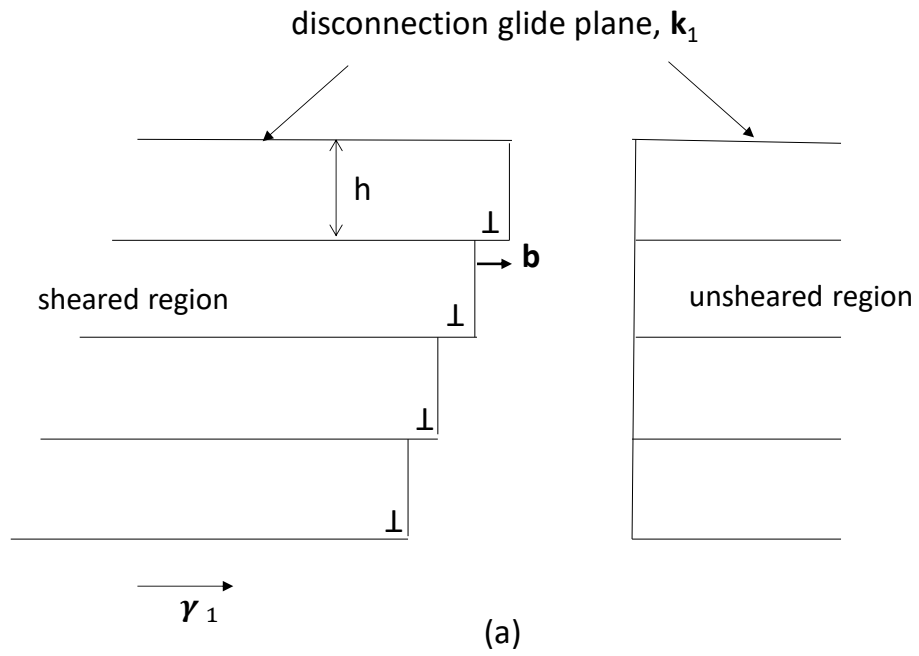
competitive mechanisms: High  $\dot{G}/\dot{N}$  favours type I  
 Low  $\dot{G}/\dot{N}$  favours type II

Type II: glide/rotation twin

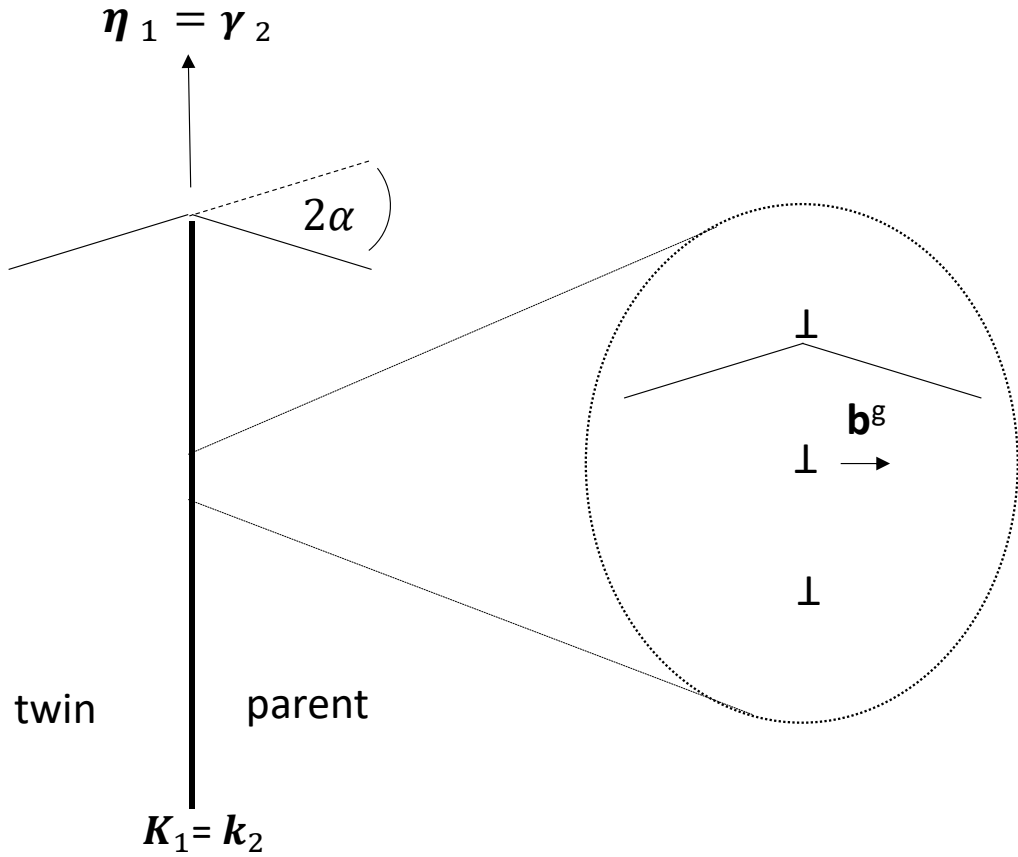




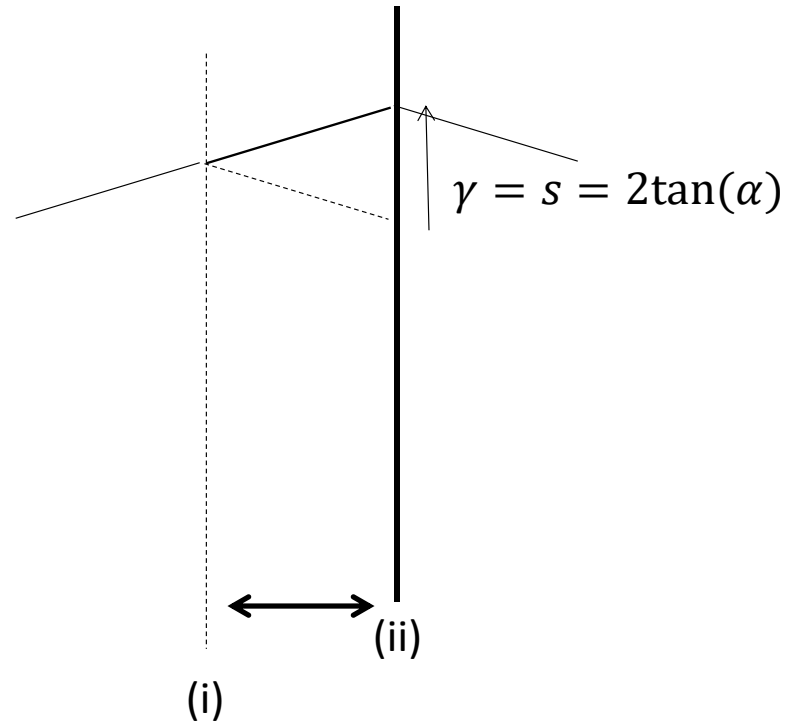
## Type II: formation of glide/rotation twin



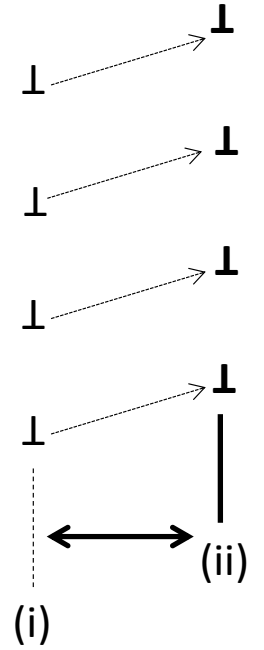
# Type II: growth



(a)



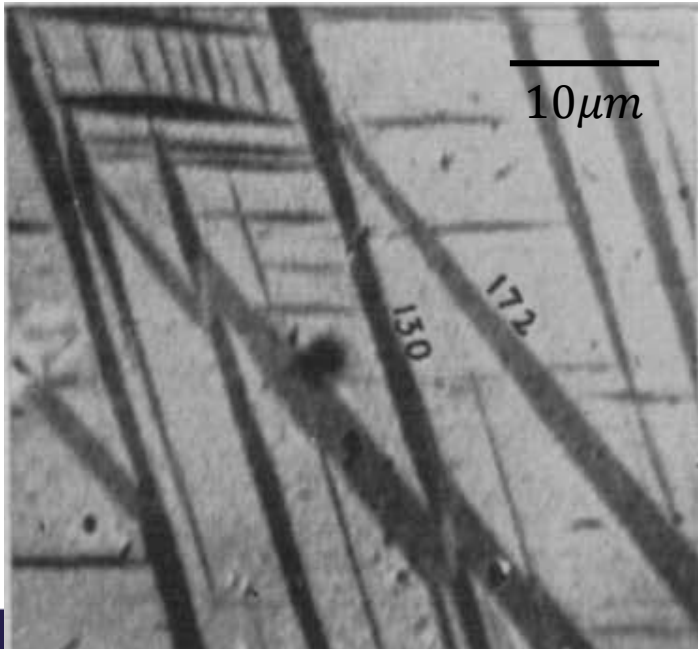
(b)



Read and Shockley, 1953

## Experimental observations: e.g. $\alpha - U$

$K_1$	$K_2$	$\eta_1$	type	$b$ nm	$h$ nm	$\gamma$	No. dist. atoms	$\dot{G}/\dot{N}$
"{17 $\bar{6}$ }"	{111}	1/2 $\langle 512 \rangle$	II	0.098	0.456	0.216	4	low
"{17 $\bar{2}$ }"	{112}	1/2 $\langle 312 \rangle$	II	0.081	0.356	0.228	4	low
{130}	{110}	1/2 $\langle 310 \rangle$	compound	0.048	0.161	0.299	2	high



$\alpha - U$ , Cahn 1953

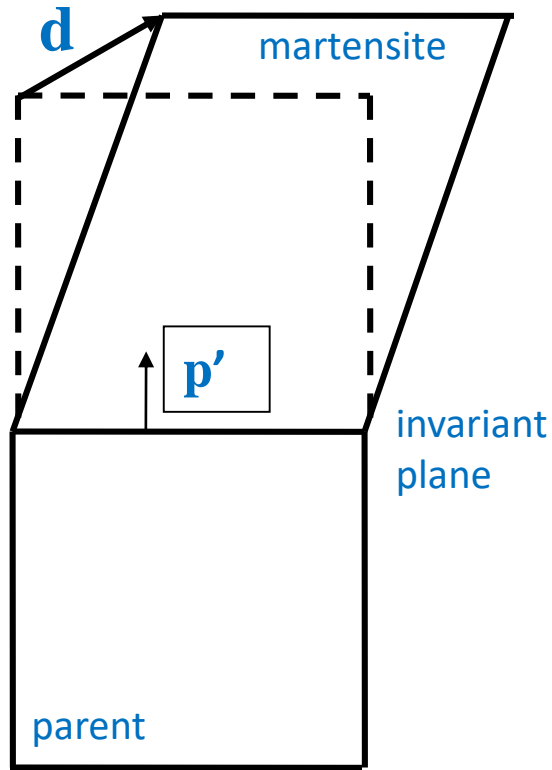
### Type II Twinning in Other Systems

NiTi  
CuAlNi  
TiPd  
devitrite



# Topological model of martensitic transformations

# PTMC

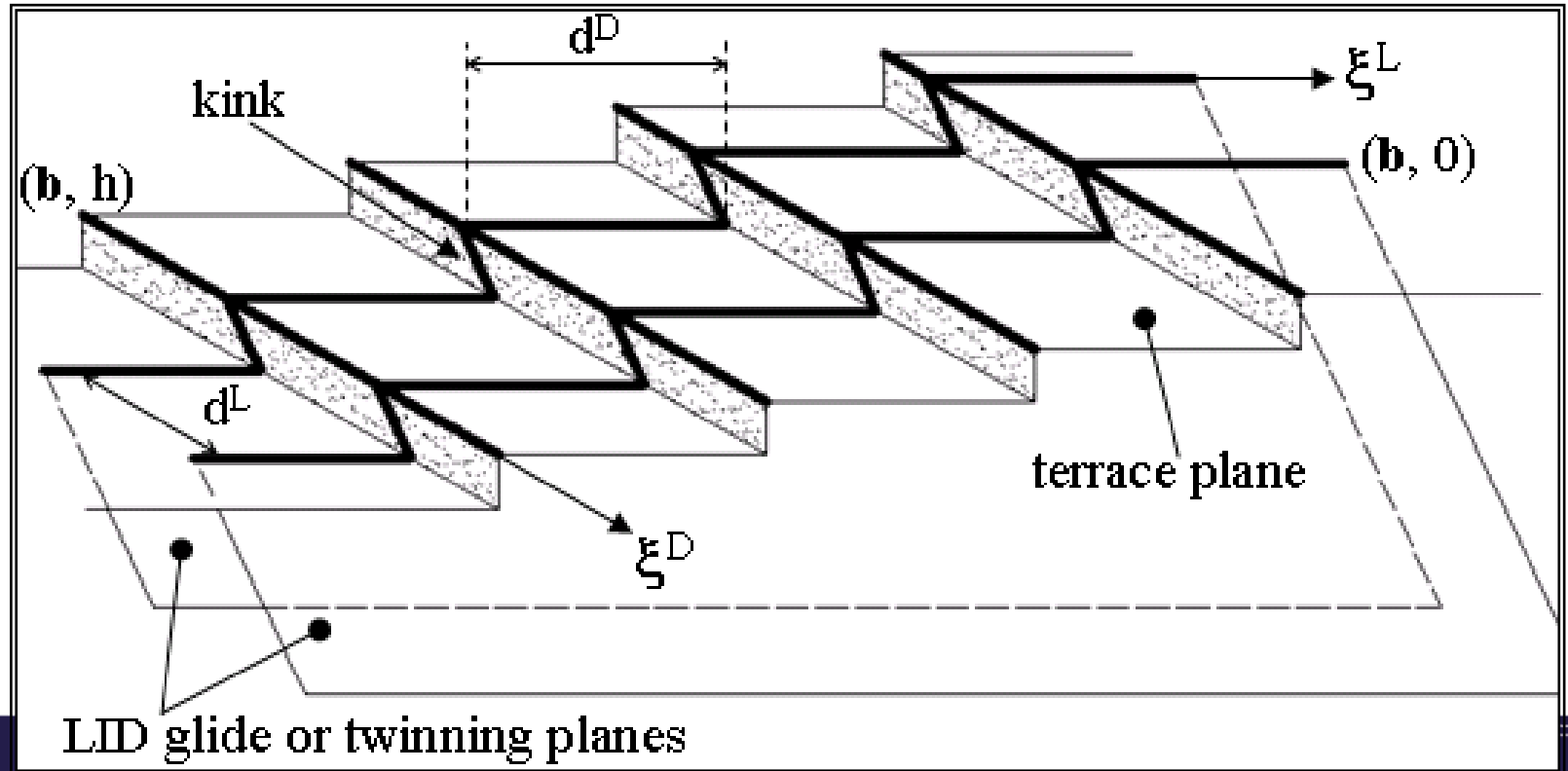


Shape deformation

$$\mathbf{P}_1 = \mathbf{RBP}_2 = (\mathbf{I} + d\mathbf{p}')$$

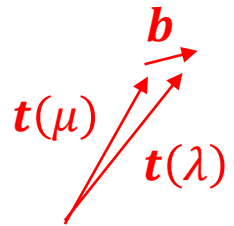
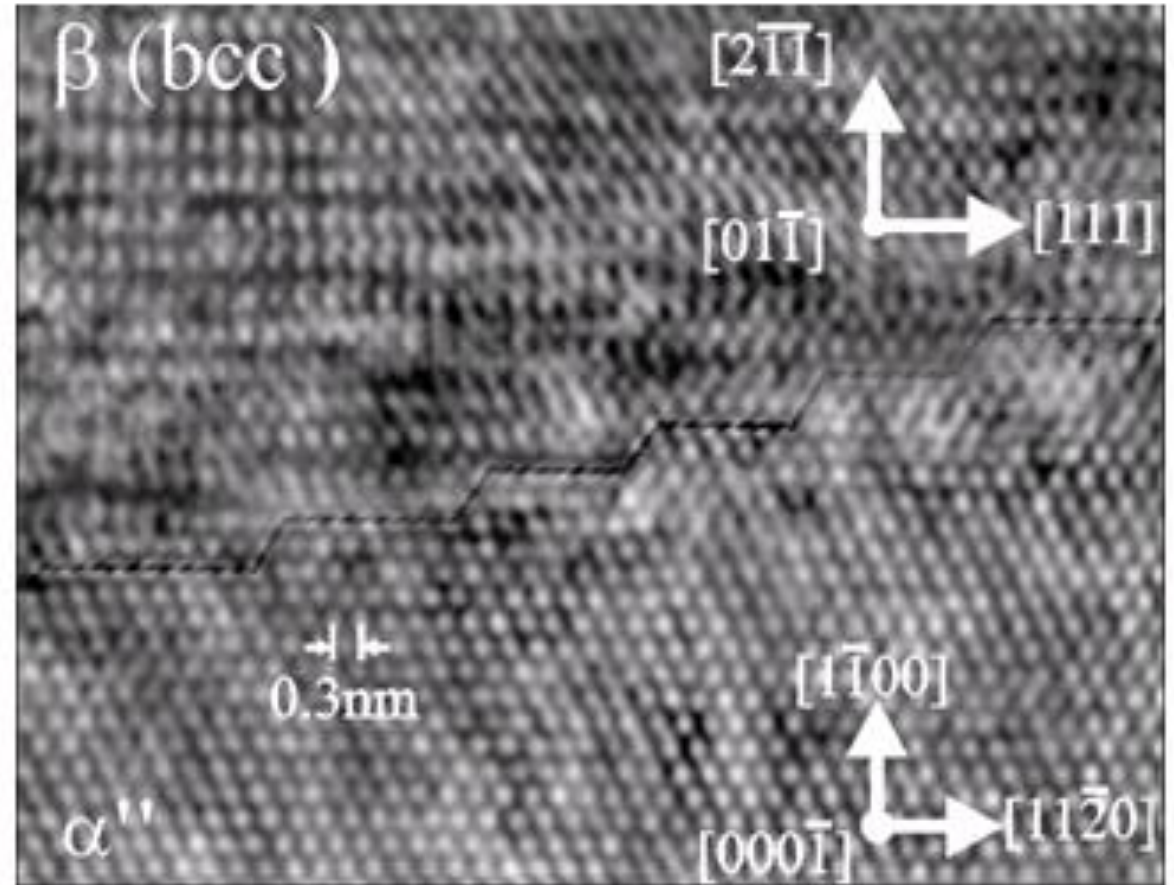
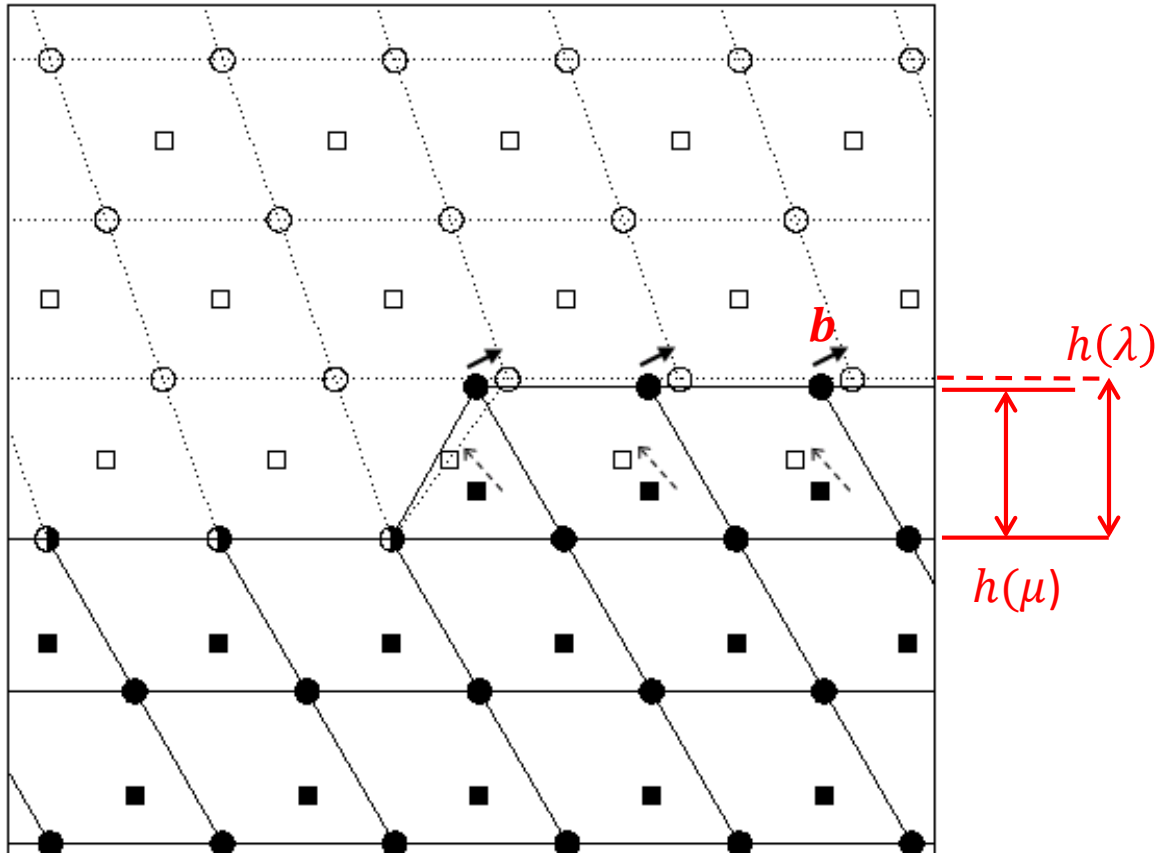
# TM

- low energy terraces (coherently strained epitaxial)
- two defect arrays: disconnections & LID
- distortion field of defect network accommodates coherency strains
- motion of all defects produces shape deformation



# Glissile Disconnections

Ti 10 wt % Mo Klenov 2002

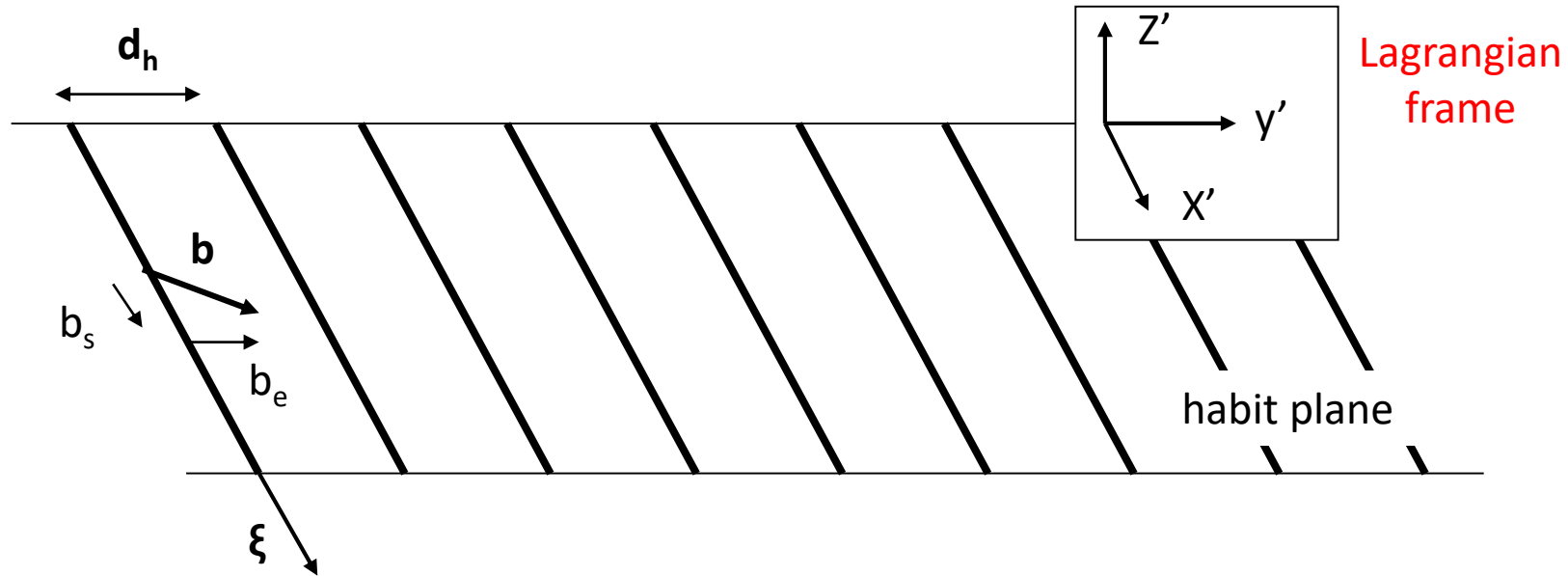


$$\mathbf{b}_n = h(\lambda) - h(\mu)$$

- 2 distinct atoms
- steps cause habit plane to be inclined to terrace plane
- $\mathbf{b}_n$  also produces rotational distortions
- motion causes one-to-one atomic exchange between phases with different densities



## Distortion field of a Defect Array

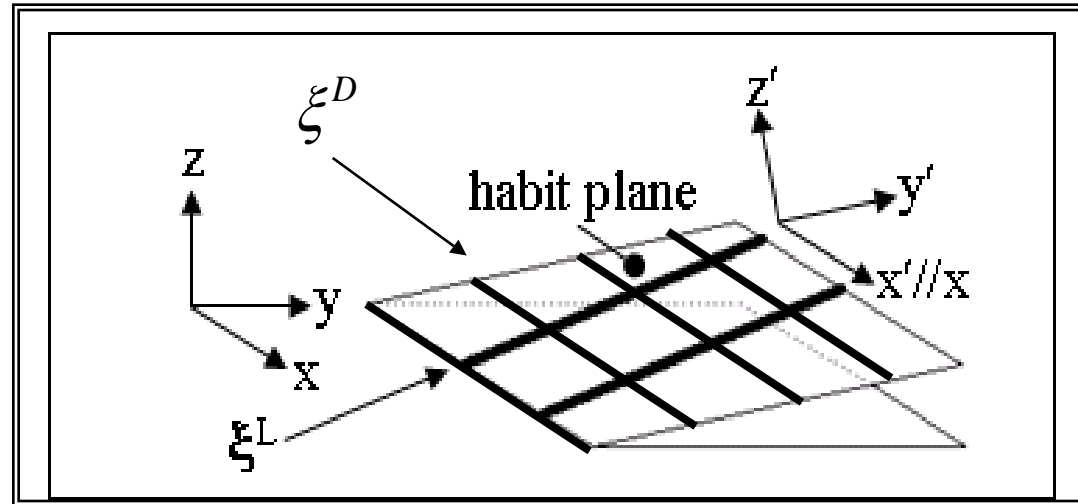


$$\mathbf{D}^m(x', y', z') = \begin{pmatrix} \epsilon'_{xx} & \epsilon'_{xy} & \epsilon'_{xz} \\ \epsilon'_{xy} & \epsilon'_{yy} & \epsilon'_{yz} \\ \epsilon'_{xz} & \epsilon'_{yz} & \epsilon'_{zz} \end{pmatrix} + \begin{pmatrix} 0 & -\omega'_{xy} & \omega'_{xz} \\ \omega'_{xy} & 0 & -\omega'_{yz} \\ -\omega'_{xz} & \omega'_{yz} & 0 \end{pmatrix}$$

$$\epsilon'_{xx} = b_x/d$$

$$\omega'_{yz} = b_z/2d$$

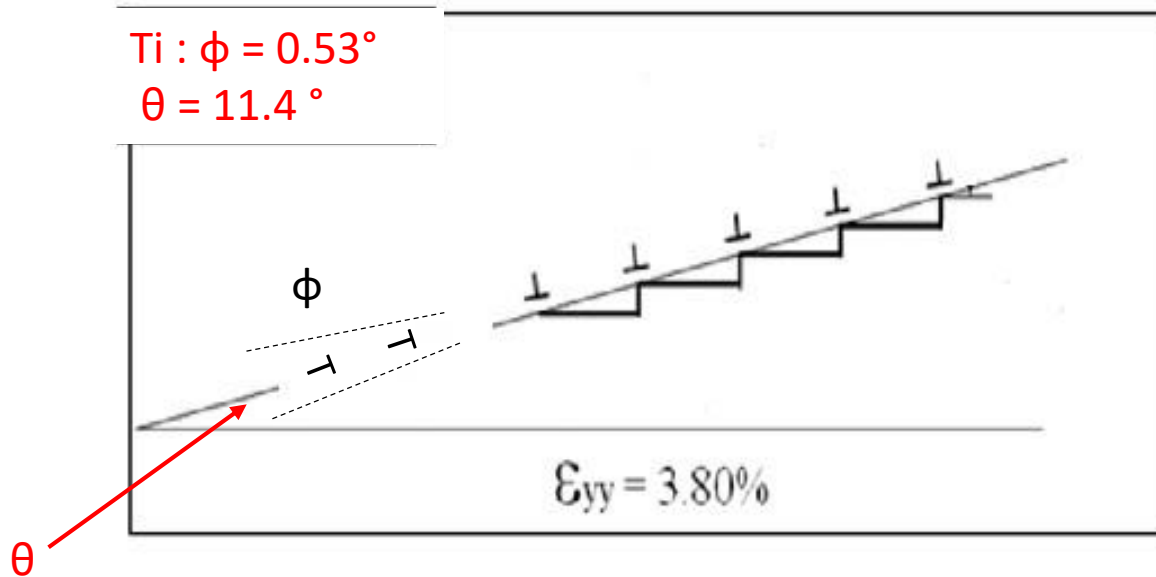
## Equilibrium: superposed coherency and defect array distortion fields



$$D_{ij}^{'m} = \begin{pmatrix} D_{xx}^{'m} & D_{xy}^{'m} & D_{xz}^{'m} \\ D_{xy}^{'m} & D_{yy}^{'m} & D_{yz}^{'m} \\ D_{xz}^{'m} & D_{yz}^{'m} & D_{zz}^{'m} \end{pmatrix} = -D_{ij}^{'c}$$

Solve the Frank-Bilby Equation for the defect array with long-range distortion matrix,  $D_{ij}^{'m}$ , which compensates  $D_{ij}^{'c}$ .

# Habit plane orientation



$\beta$  crystal:  $\Theta - \phi$

$\alpha$  crystal:  $\Theta + \phi$

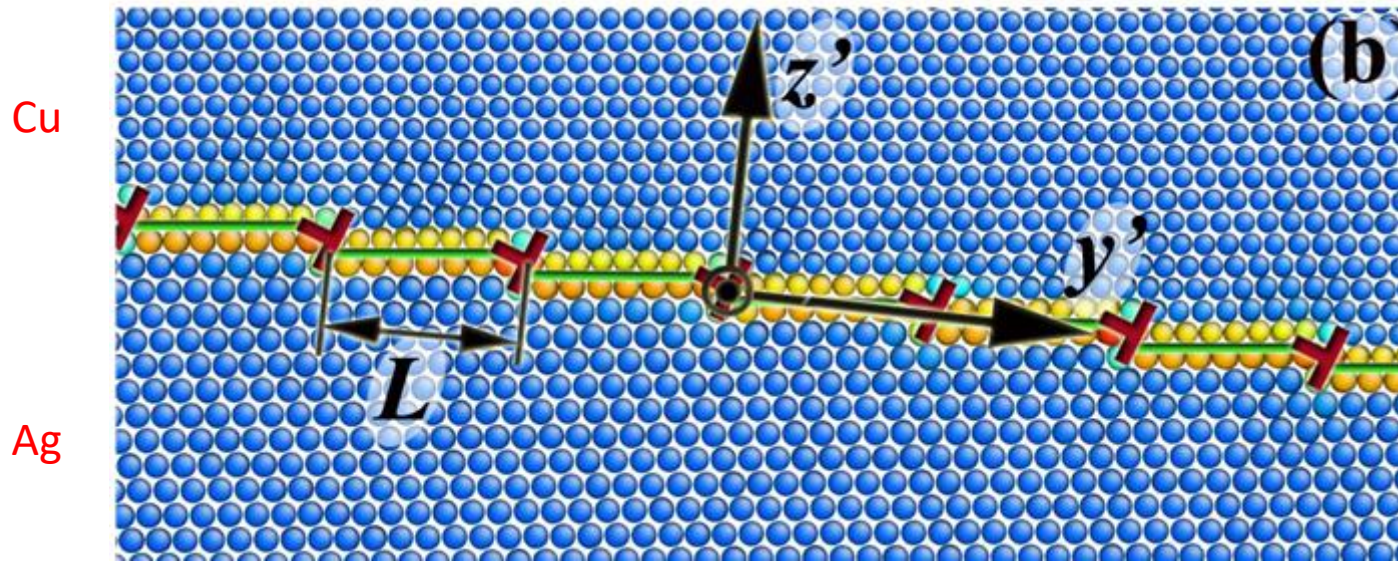
homogeneous  
isotropic  
approximation

inhomogeneous anisotropic case  
rotations partitioned according to relative elastic  
compliances

TM solutions for habit plane orientation differ slightly from PTMC, unless  $\mathbf{b}_n = 0$



# Partitioning of rotations

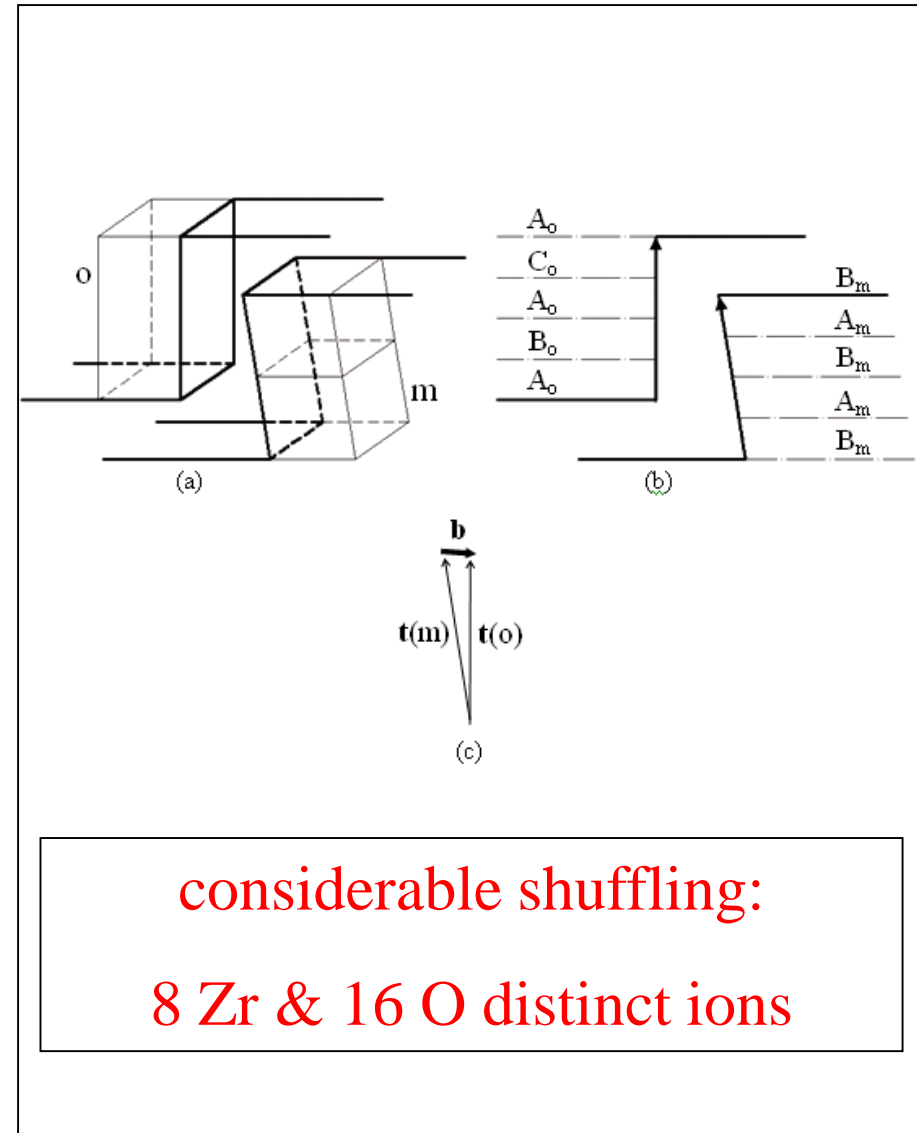
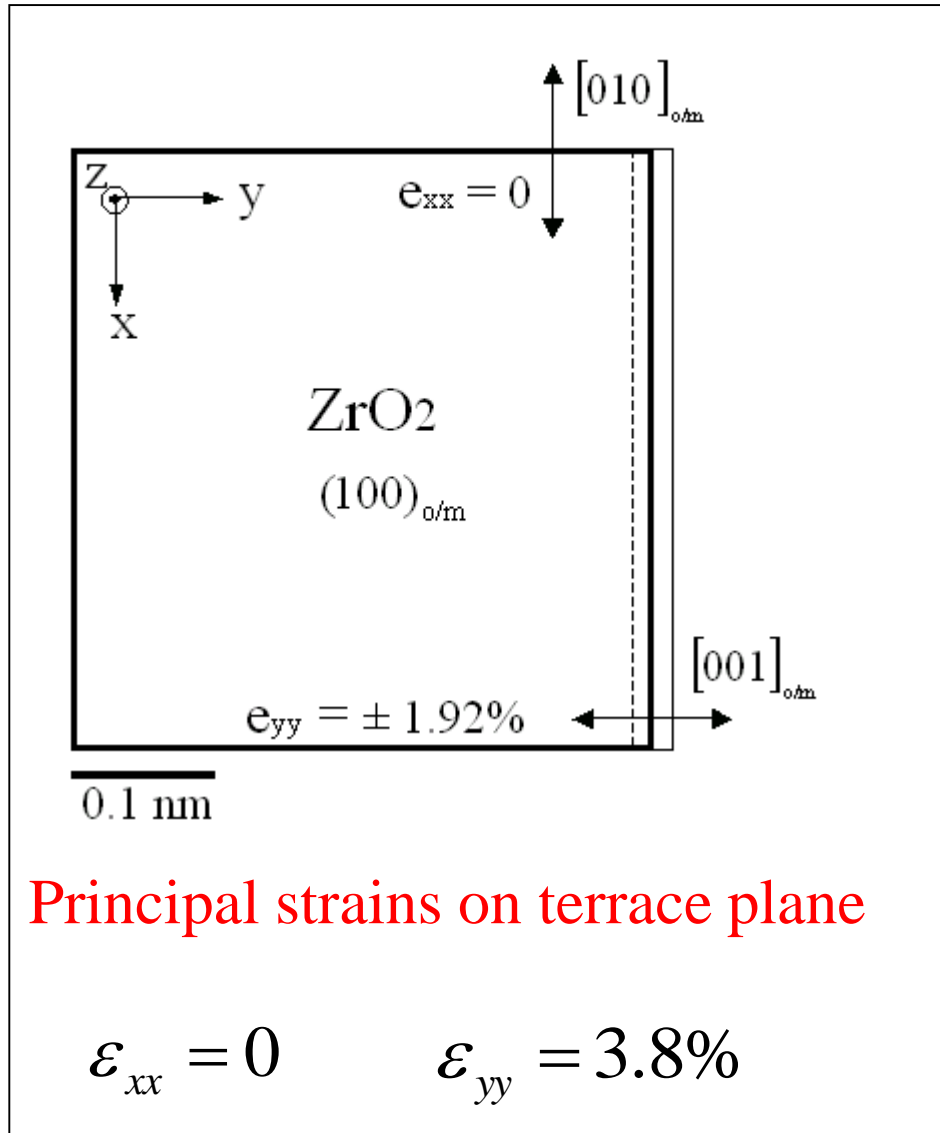


$$\epsilon_{yy}^c = 12.33\%$$

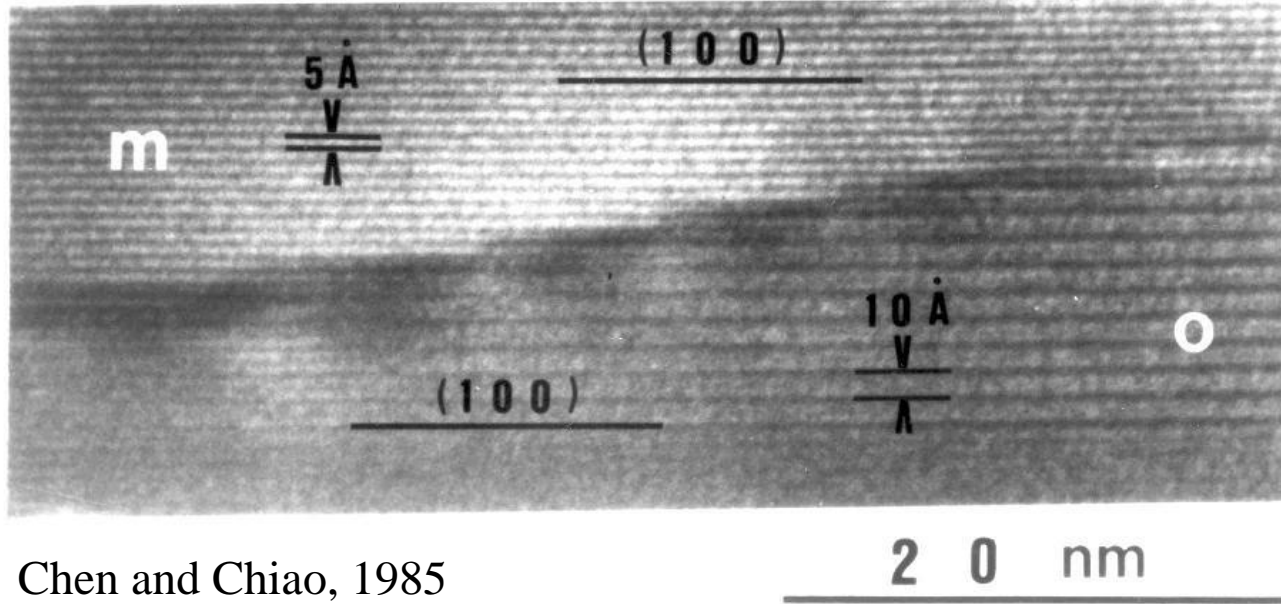
molecular dynamic simulation of static Cu(111)/Ag(111) interface, Wang et al. 2011

Case	$\varphi_{Cu}$	$\varphi_{Ag}$	$\varphi$	$-\varphi_{Ag}/\varphi_{Cu}$
Isotropic, inhomogeneous	0.449	-0.698	1.15	1.55
Anisotropic	0.504	-0.853	1.36	1.69
MD	0.483	-0.929	1.41	1.92
MD (Artificial)	0.665	-0.659	1.312	0.97

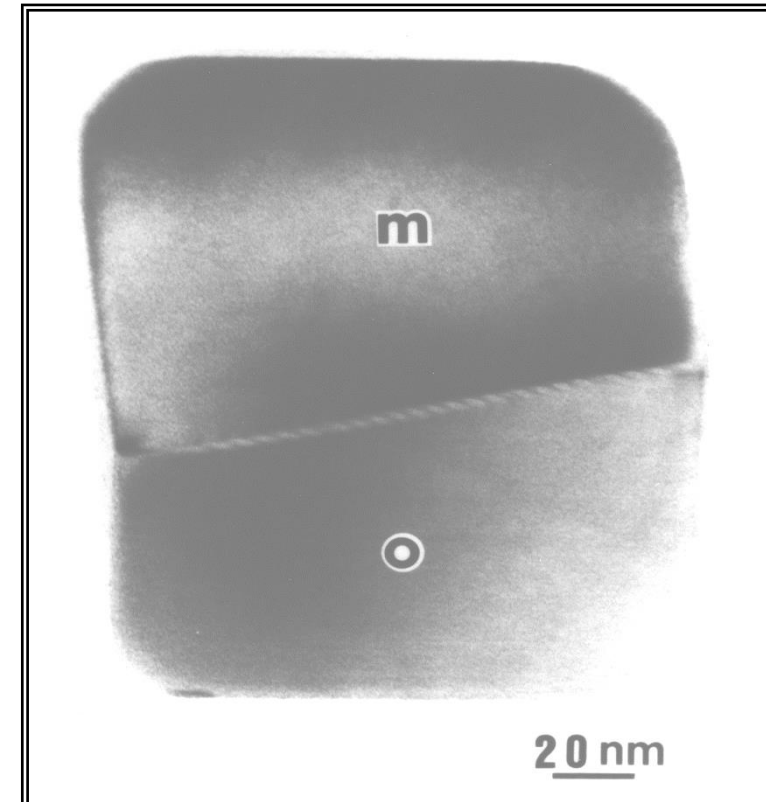
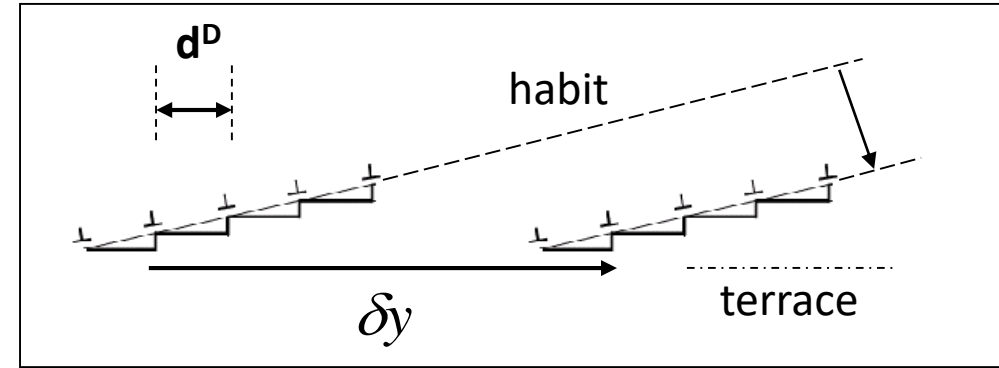
# Orthorhombic to Monoclinic Transformation in $\text{ZrO}_2$



# synchronous motion of disconnections



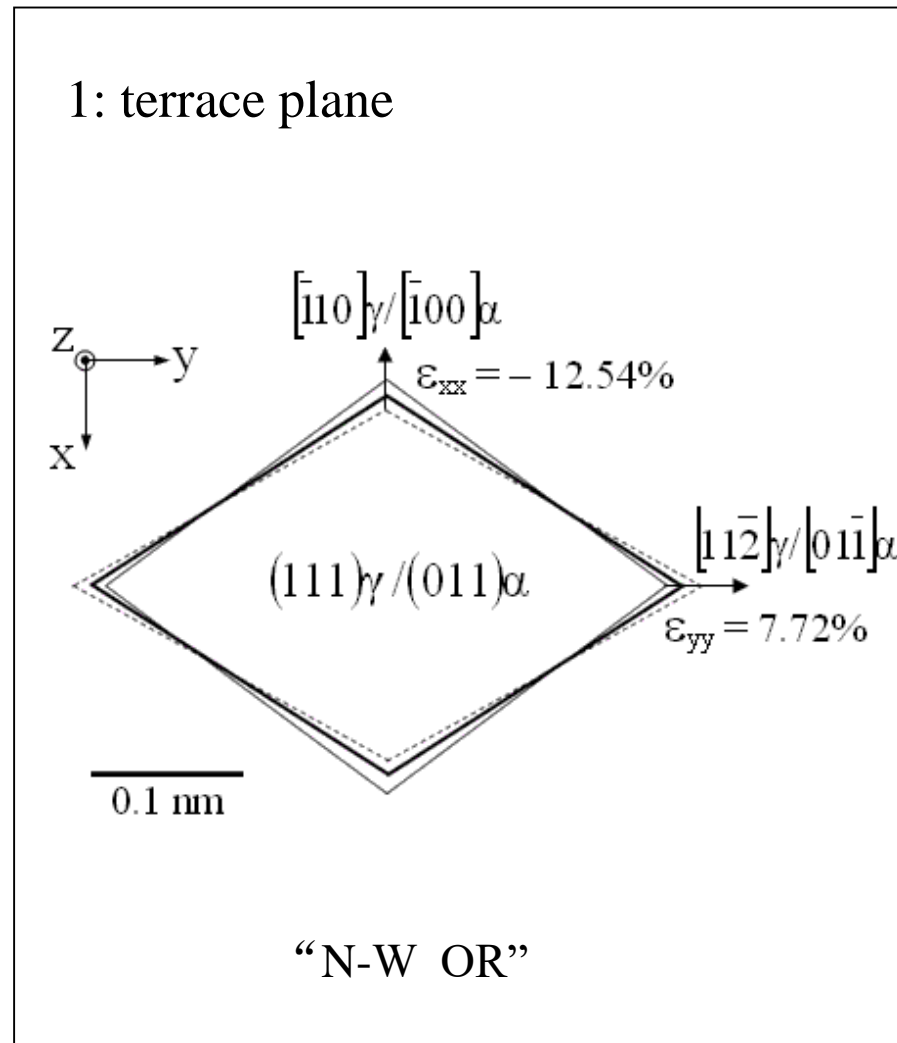
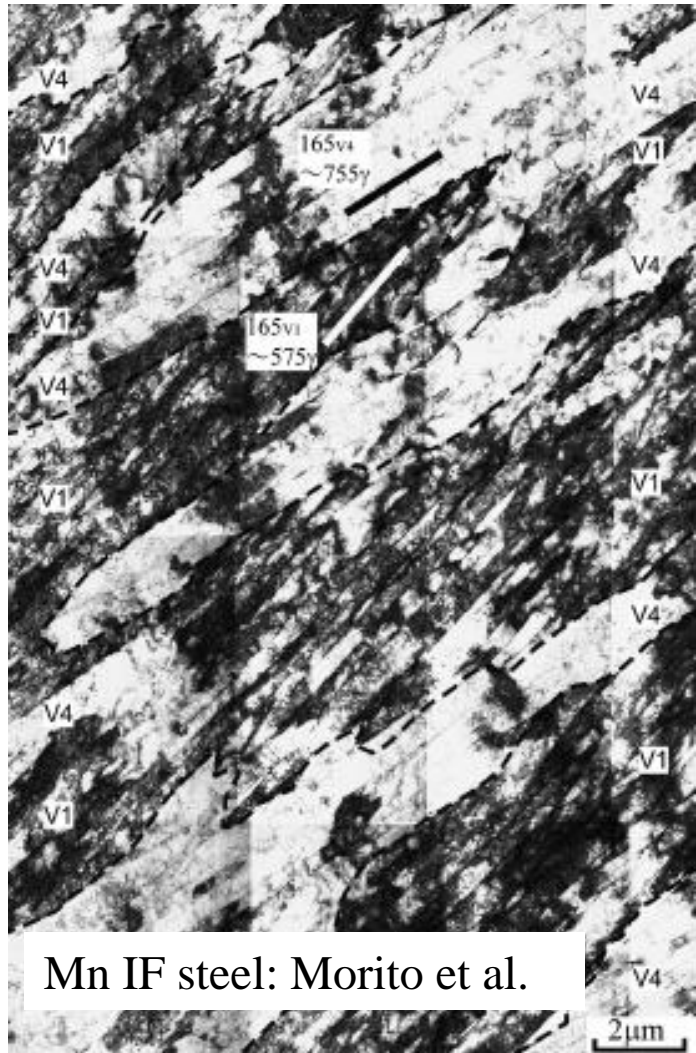
Chen and Chiao, 1985



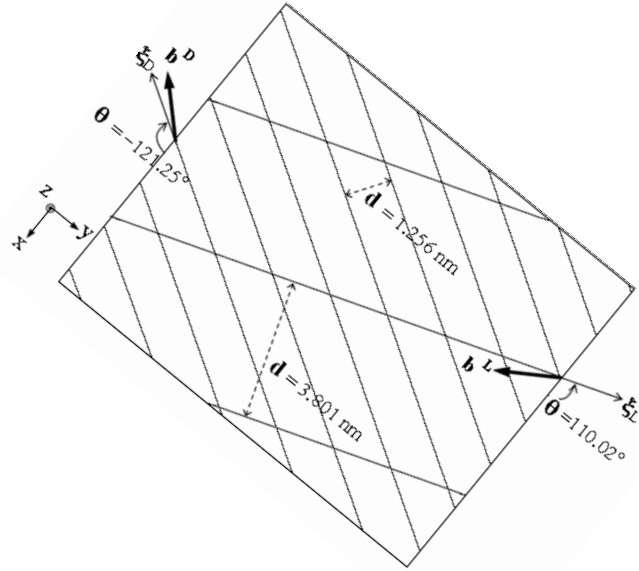
$$\Gamma_m^D = \begin{pmatrix} 0 & 0 & \gamma_{xz} \\ 0 & 0 & \gamma_{yz} \\ 0 & 0 & \varepsilon_{zz} \end{pmatrix} = \frac{\delta y}{d^D} \begin{pmatrix} b_x \\ b_y \\ b_z \end{pmatrix}^D (0 \quad 0 \quad n_z)$$



# Lath martensite in ferrous alloys

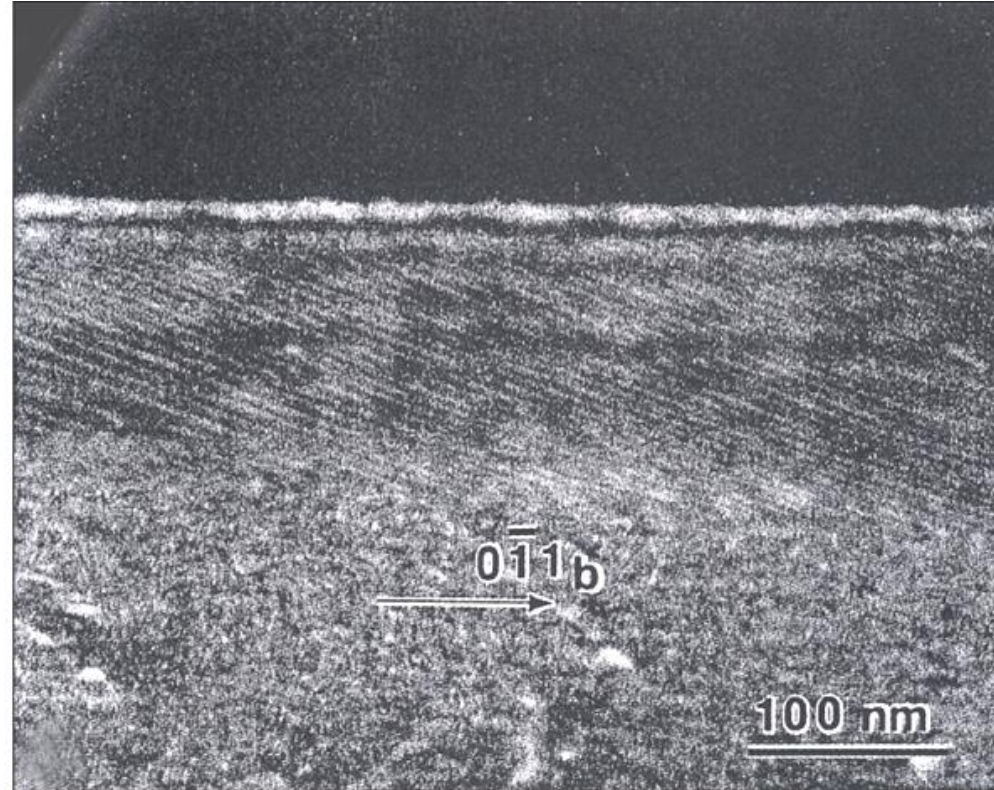


## TEM: LID slip dislocations



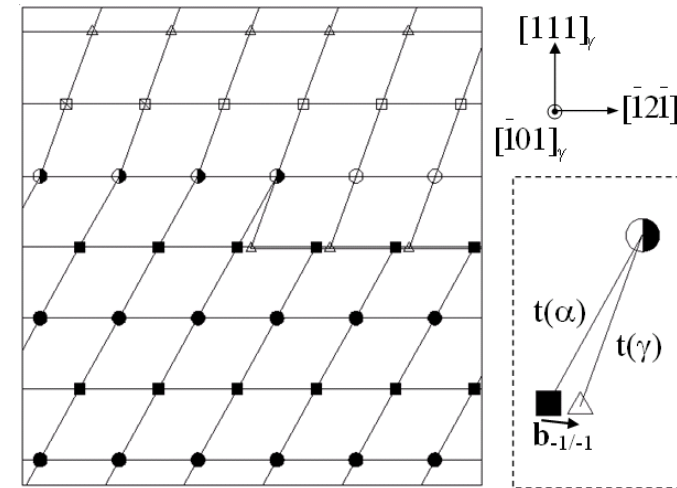
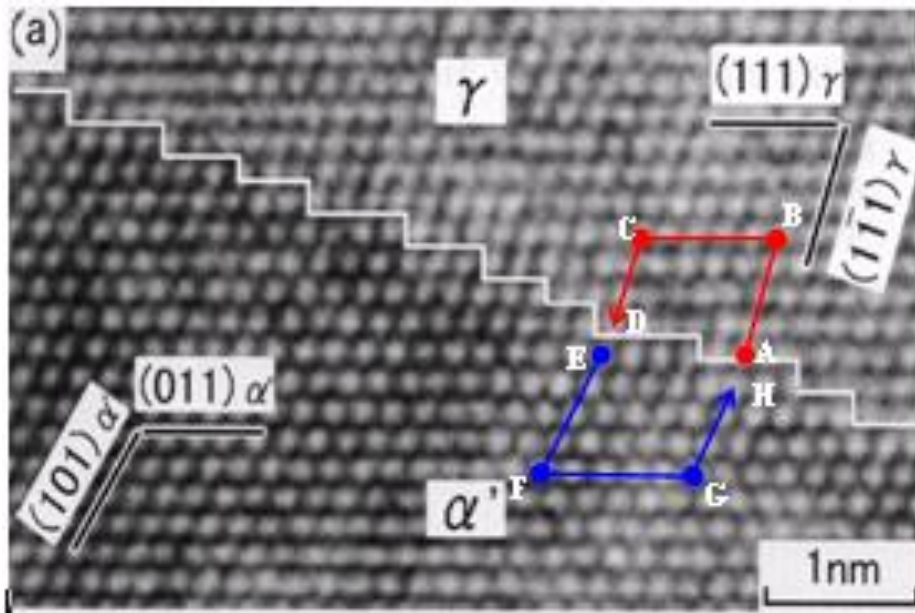
~{575}

G-T OR



$1/2[1\bar{1}1]_{\alpha}$  dislocations,  $\sim 10^{\circ}$  from screw, with  
spacing 2.8 -6.3 nm  
Fe-20Ni-5Mn (Sandvik and Wayman, 1983)

# TEM: Disconnections in near screw orientation



Moritani et al. Fe-Ni-Mn

$[-101]_{\gamma}$  projection



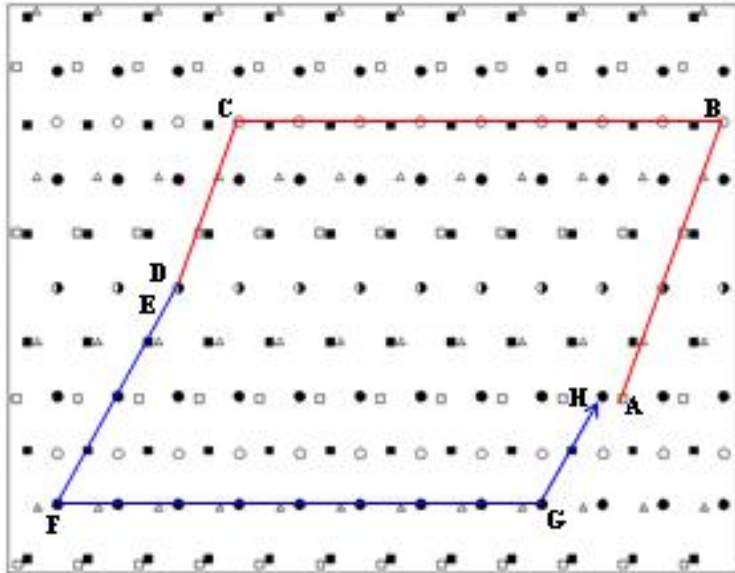
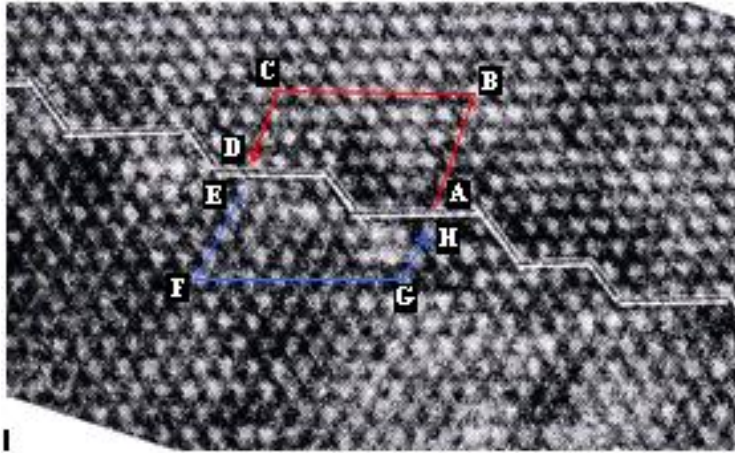
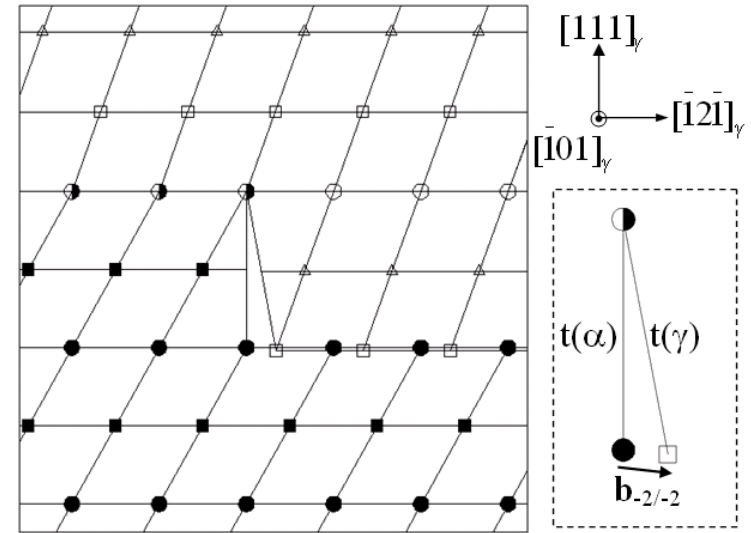


## Plate Martensite

$$\sim\{121\}$$



Ogawa and Kajiwara, 2004

Fe-Ni-Mn

# Conclusions

Topological modelling provides insights into mechanisms and kinetics.

Twining:

- ❖ proposed new model of type II twin formation.

Martensite:

- ❖ predicted interface structures consistent with observations,
- ❖ predicted habits differ slightly from PTMC.

